From Knowledge to Wisdom

ISSN 1934-7359 (Print)
ISSN 1934-7367 (Online)
DOI:10.17265/1934-7359

Journal of Civil Engineering and Architecture

Volume 15, Number 6, June 2021

David Publishing Company
www.davidpublisher.com

Journal of Civil Engineering and Architecture

Volume 15, Number 6, June 2021 (Serial Number 163)

David Publishing Company
www.davidpublisher.com

Publication Information:
Journal of Civil Engineering and Architecture is published monthly in hard copy (ISSN 1934-7359) and online (ISSN 1934-7367) by David Publishing Company located at 3 Germay Dr., Unit 4 #4651, Wilmington DE 19804, USA.

Aims and Scope:
Journal of Civil Engineering and Architecture, a monthly professional academic journal, covers all sorts of researches on structural engineering, geotechnical engineering, underground engineering, engineering management, etc. as well as other issues.

Manuscripts can be submitted via Web Submission, or e-mailed to civil@davidpublishing.com or civil@davidpublishing.org. Submission guidelines and Web Submission System are available at http://www.davidpublisher.com.

Editorial Office:
3 Germay Dr., Unit 4 #4651, Wilmington DE 19804, USA
Tel:1-323-984-7526; Fax:1-323-984-7374
E-mail: civil@davidpublishing.com; civil@davidpublishing.org; shelly@davidpublishing.com

Abstracted/Indexed in:
Cambridge Science Abstracts (CSA)
Ulrich's Periodicals Directory
Chinese Database of CEPS, Airiti Inc. & OCLC
Summon Serials Solutions, USA
China National Knowledge Infrastructure (CNKI)
Turkish Education Index
Google Scholar
ProQuest, USA
J-Gate

Subscription Information:
$720/year (print)

David Publishing Company
3 Germay Dr., Unit 4 #4651, Wilmington DE 19804, USA
Tel:1-323-984-7526; Fax:1-323-984-7374
E-mail: civil@davidpublishing.com; civil@davidpublishing.org; shelly@davidpublishing.com
Digital Cooperative Company: www.bookan.com.cn

David Publishing Company
www.davidpublisher.com

Journal of Civil Engineering and Architecture

Volume 15, Number 5, May 2021 (Serial Number 162)

Contents

Journal of Civil Engineering and Architecture 15 (2021) 285-293
doi: 10.17265/1934-7359/2021.06.001

Influence of Non-uniform Elevated Temperature on the Structural Stability and Strength of Gypsum-Sheathed Cold-Formed Steel Beam Channel Members

Elias Ali[1], Kermelos Woldeyes[2] and Girum Urgessa[3]

1. Department of Civil and Environmental Engineering, The University of Alabama in Huntsville, Huntsville, AL 35805, USA

2. Department of Civil, Architectural and Environmental Engineering, Drexel University, Philadelphia, PA 19104, USA

3. Department of Civil, Environmental and Infrastructural Engineering, George Mason University, Fairfax, VA 22030, USA

Abstract: The objective of this paper is to computationally explore the structural stability and strength of gypsum-protected CFS (cold-formed steel) beam channel sections under non-uniform elevated temperatures when exposed to standard fire on one side of the panel and subjected to pure bending. When a CFS member is subjected to fire (or thermal gradients) its material properties change—but this change happens around the cross-section and along the length creating a member which is potentially non-uniform and unsymmetrical in its response even if the apparent geometry is uniform and symmetric. Computational finite element models were analyzed in ABAQUS to establish steady-state thermal gradients of interest. Existing test data were utilized to develop the temperature dependence of the stress-strain response. The time-dependent temperature distribution on the cross-sections obtained from heat transfer analysis was later used in the stability and collapse analyses. The stability of the models was explored to characterize how local, distortional, and global buckling of the member evolves under both uniform and non-uniform temperature distributions. Finally, collapse simulations were performed to characterize the strength under pure bending and explore directly the evolution of strength under the influence of non-uniform temperature.

Key words: CFS, non-uniform temperature distribution, stability, collapse moment.

1. Introduction

The investigation of fire safety and responses of structures under elevated temperature has gained increased research interest in the last two decades due to the increased incidents of major fires and fire accidents in buildings, building compartments, and infrastructure. Recently, CFS (cold-formed steel) is extensively used from low to medium raised structures, namely for residential, industrial, and commercial buildings as the framing, partition walls, and exterior walls and even as a load-bearing structural component system on the floor and ceilings. This growing interest in thin-walled structural members in general and CFS, in particular, is due to their unique advantage of high strength to weight ratio. During fire accidents, steel would quickly heat up and results in a rapid reduction in its mechanical properties, particularly the yield strength and stiffness. These reductions in mechanical properties have been investigated by researchers such as Keerthan and Mahendran [1], Kankanamge [2], and Cheng et al. [3] both experimentally and numerically. It was found that the reductions in strength and stiffness are even more significant in CFSs. Therefore, CFS members are commonly used in structural wall and floor systems protected with gypsum board, with or without insulation, on both sides for fire protection.

Past researchers such as Kankanamge [2], Alfawakhiri and Farid [4], Shahbazian and Wang [5] have investigated the buckling behavior and resistance of CFS members at elevated temperatures. Yin and

Corresponding author: Elias Ali, Ph.D., lecturer, research fields: fire and blast safety of structures, composite materials.

Wang [6] investigated the effect of non-uniform temperature distribution on lateral-torsional buckling resistance of steel I-beams using parametric study. Alfawakhiri and Sultan [7] studied the fire resistance of load-bearing LSF (light gauge steel frame) assemblies using analytical thermo-structural model procedures to simulate lateral deformation histories and predict structural failure time. They considered the gypsum board and three different types of insulations (glass, rock, and cellulose) to determine the temperature profiles on the LSF steel stud and the failure time of the wall. Sultan et al. [8] provided a model for predicting heat transfer through insulated steel-stud wall assemblies exposed to fire on one side of the panel. To verify their model, they performed tests on four full-scale wall assemblies with insulation in the wall cavity. They considered two cases of gypsum board (single layer and two layers of gypsum at both ends). Kontogeorgos et al. [9] developed a model to simulate the temperature distribution in the wall assembly of the gypsum board using the ISO834 fire curve. Kukuck [10] studied heat and mass transfer through gypsum partition subjected to fire exposure. The developed model incorporates the mass transport effects of water in both liquid and vapor form and found that this mass transport plays a significant role in the thermal response of gypsum wallboard when subjected to fire. The application of a new composite material called functionally graded material for thermal sheathing in thin-walled structures was investigated by Ali and Bayleyegn [11]. Analytical and numerical buckling analysis of composite plates made of metal and ceramic plates was also studied by Ali and Bayleyegn [12] for extreme loading application.

During a fire, the temperature distribution along the CFS section is usually assumed to be uniform, for analytical simplicity, both across the section and along the member length. Thus, buckling behavior is analyzed based on uniform reduced material properties. However, in a real fire scenario, the temperature distribution in a CFS section is generally not uniform. This is especially true when the CFS structural member is exposed to fire only on one side. This phenomenon would make buckling behavior and analysis more complicated than the commonly practiced analysis approach.

Thus, this paper presents the analysis that adds to the state-of-the-art in understanding the effect of non-uniform elevated temperature distributions on the structural buckling behavior and responses of a CFS beam under pure bending due to fire on one side of the panel.

2. Modeling Approach and Thermal Analysis

Evaluating the non-uniform temperature distribution in the CFS channel cross-section, which is protected by the gypsum board, requires heat transfer analysis. Commonly, these temperature distributions are performed using finite element analysis. However, this approach would consume time and high storage capacity when there is a need to perform a parametric study. Thus, three separate input scripts for 2-D time-dependent heat transfer analysis, elastic buckling analysis, and non-linear collapse analysis were developed using a MATLAB program, which is then coupled with a finite element package ABAQUS. The fire temperature used in the heat transfer analysis was defined using the ISO834 (International Organization for Standardization 834) standard fire curve given by Eq. (1), where T_a = 20 °C is the ambient temperature and t is time in seconds.

$$T = T_a + 345\log(8t/60+1) \quad (1)$$

Fig. 1 shows the ISO standard fire curve used in the study, the configuration of the CFS, and a 12.5 mm gypsum board on both exposed and unexposed sides of the structural member. Material properties used in the heat transfer were density, thermal conductivity, and specific heat for both steel and gypsum boards.

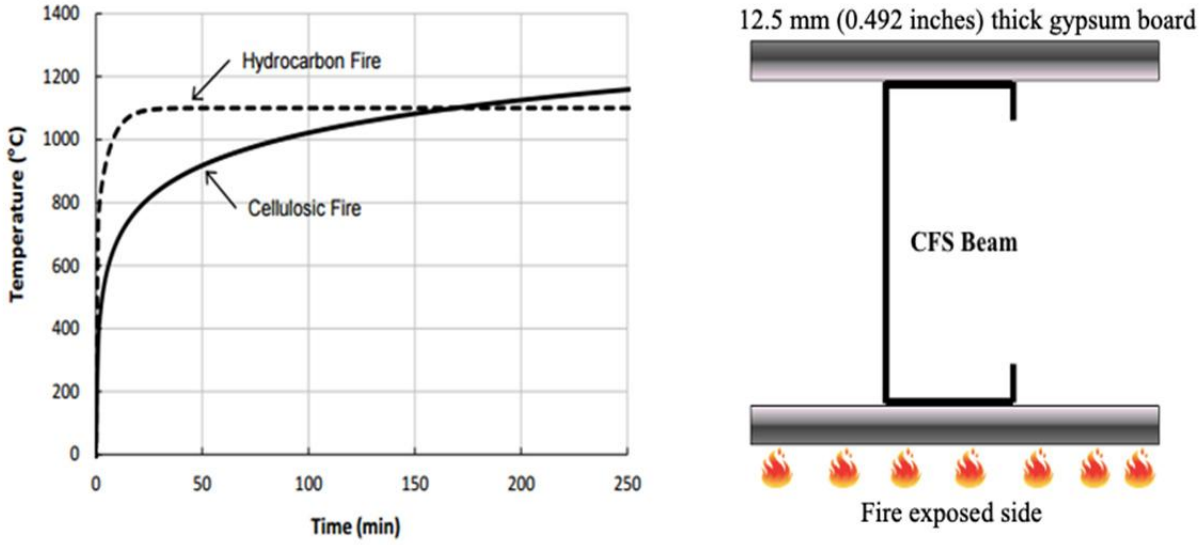

(a) (b)

Fig. 1 (a) ISO834 standard fire and (b) CFS channel section protected by gypsum board and fire on one side.

Table 1 Material properties used in the heat transfer analysis.

Material	Density (kg/m^3)	Thermal conductivity (W/m·°C)	Specific heat (J/kg·°C)
Steel	7,850	$\lambda = 54 - 3.33 \times 10^{-2}(T)$ (20 °C ≤ T < 800 °C) $\lambda = 27.3$ (800 °C ≤ T ≤ 1,200 °C)	$c = 425 + 7.73 \times 10^{-1}(T) - 1.69 \times 10^{-3}(T^2) + 2.22 \times 10^{-6}(T^3)$ (20 °C ≤ T < 600 °C) $c = 600 + \frac{13{,}002}{738 - T}$ (600 °C ≤ T < 735 °C) $c = 545 + \frac{17{,}820}{T - 731}$ (735 °C ≤ T ≤ 900 °C)
Gypsum board	727	0.2 at 10 °C 0.218 at 150 °C 0.103 at 155 °C 0.3195 at 1,200 °C	925.04 at 10 °C 941.5 at 95 °C 24,572.32 at 125 °C 953.14 at 155 °C 1,097.5 at 900 °C

These values vary with temperatures and a range of values were suggested by several researchers. In this paper, the values obtained from Feng et al. [13] were used as shown in Table 1.

Heat transfer analysis and structural behavior investigation were carried out for three CFS sections (362S200-54, 400S200-54, and 600S200-54). The thermal boundary conditions considered during the heat transfer analysis were convection and radiation for both fire exposed sides and ambient sides. These interaction properties were defined by convection surface film coefficient of 25 W/m^2·K and 10 W/m^2·K for the exposed side and ambient side respectively. Radiation film coefficient of 25 W/m^2·K for fire exposed side, and emissivity of 0.3 and 0.8 for fire exposed and ambient sides were used respectively.

Fig. 2 shows the temperature profile for CFS beam channel section 400S200-54 (web height = 4 inches, flange width = 2 inches, and design thickness = 0.0556 inches) sheathed with a single-layer gypsum board after 60 min of fire. It was observed that the temperature in the web elements of the CFS section is not uniform with the highest temperature at parts closer to the fire exposed side and gradually tends to

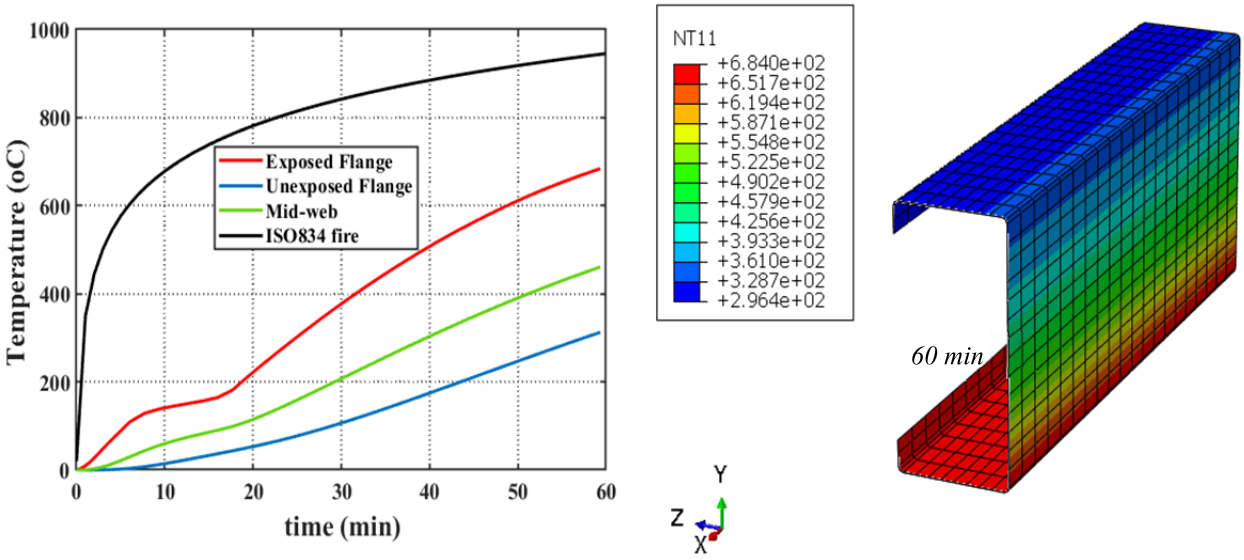

Fig. 2 Temperature distribution on 400S200-54 CFS section after 60 min of fire.

attain smaller temperature at the unexposed surface. The temperature in the unexposed flange and lip remains relatively low even after 60 min of fire exposure, compared to the fire exposed flange and lip.

3. Model Details and Assumptions

3.1 Mechanical Properties of CFS at Elevated Temperatures

When CFS structural members are exposed to fire or elevated temperature, there will be a rapid increase in temperature in the member which causes a significant reduction in mechanical properties, particularly its stiffness, yield strength, and coefficient of thermal expansion. These reductions would facilitate the collapse of the member or the entire structure at a critical temperature and loadings.

Many researchers carried out experimental tests on different steel sections and grades and developed equations for predicting the reduction in the mechanical properties of steel at elevated temperatures. Gerlich [14] derived an equation for yield strength and elastic modulus for a temperature range below 650 °C using several data from steady-state experimental tests. Chen and Young [15] investigated the mechanical properties of CFSs at elevated temperatures for both steady and transient tensile coupon tests for a temperature range of up to 1,000 °C for two steel grades of G550 and G500 with a plate thickness of 1.0 and 1.9 mm respectively. They proposed two mechanical properties reduction equations for yield strengths and elastic modulus, both normalized at ambient temperature properties.

This paper uses the recent experimental results from Kankanamge [2] who modified the previous results from Ranawaka and Mahendran [16] and proposed predictive equations for both high and low-grade steel types. The reduction factors in Table 2 were used for elastic buckling and collapse analyses.

3.2 Boundary Conditions and Loading in the Model

A simply supported CFS beam member subjected to pure bending was used in both elastic and non-linear collapse analysis. Four node S4R5 type shell elements were used in both elastic and non-linear collapse analysis of the CFS. This selection was based on the sensitivity study performed for different mesh types and sizes. At both ends of the beam, longitudinal (u_1) and transverse (u_3) deformations, and twisting in the minor axis (u_{R2}) were restrained in the analysis as shown in Fig. 3.

Table 2 Reduction factors of mechanical properties of CFS at elevated temperature.

Temperature (°C)	20	100	200	300	400	500	600	700	800
$k_{yT} = (f_{y,T}/f_{y,20})$	1	0.999	0.990	0.952	0.694	0.391	0.111	0.070	0.030
$k_{ET} = E_T/E_{20}$	1	0.933	0.849	0.715	0.580	0.445	0.310	0.175	0.040

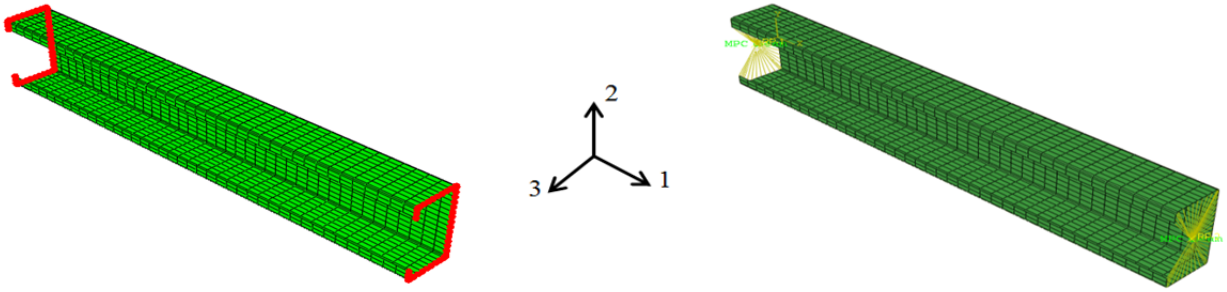

Fig. 3 Boundary condition on CFS beam.

4. Results and Discussion

4.1 Effect of Temperature Distribution on the Stability of CFS Beam

Both uniform and non-uniform temperature distributions were investigated for the three CFS sections. A uniform temperature in the CFS section means the whole cross-section was assumed to have the same temperature for each analysis step while for non-uniform temperature distribution cases predefined thermal gradient from the heat transfer outputs was used for each time step for the stability analysis of the CFS beams. Stress due to unit concentrated moment was then applied at the simply supported end to analyze the elastic buckling analysis. This process was repeated for all three sections with 11-time steps, which range from 37 °C to 600 °C and beam length from 5-400 inches, a total of 264 separate analyses for each beam. The critical buckling moment and normalized critical buckling moment results for the three CFS sections are presented in Figs. 4-7. The elastic critical buckling analyses for all the three sections in both uniform and non-uniform temperature distributions considered clearly show the reduction in critical buckling moments with increased fire temperature. These reductions also exhibit the same pattern for the reduction in material properties mainly the modulus of elasticity. It has a small or gradual reduction until the maximum flange temperature reaches 250 °C and follows with a step-change in capacity up to 600 °C, it then starts to exhibit a gradual change in moment capacity. These observed temperatures are consistent with the changes in mechanical properties listed in Table 2.

The critical moment for all three sections exhibits mainly two buckling modes for all temperature ranges: local buckling and distortional. The local buckling mode was predominant for the half wavelength of up to 5 inches where the minimum elastic critical moment was observed after the maximum elevated temperature on the exposed flange reaches 250 °C and beyond. The distortional buckling mode was predominant at a half wavelength of 12 inches and above. A combination of both local and distortional buckling modes was observed in the intermediate member lengths between 6-12 inches. It was also observed that using a non-uniform temperature distribution in the stability analysis significantly increases the section's critical buckling moment compared to the uniform temperature cases. The reason for such behavior can also be explained by an increase in rigidity at both compressions flanges and lips, due to relatively lower temperature at the non-exposed side, which would directly affect the compression stresses at the flanges, resulting in a higher buckling moment. Also, an increase in section web would increase the critical buckling moment as shown in Fig. 7.

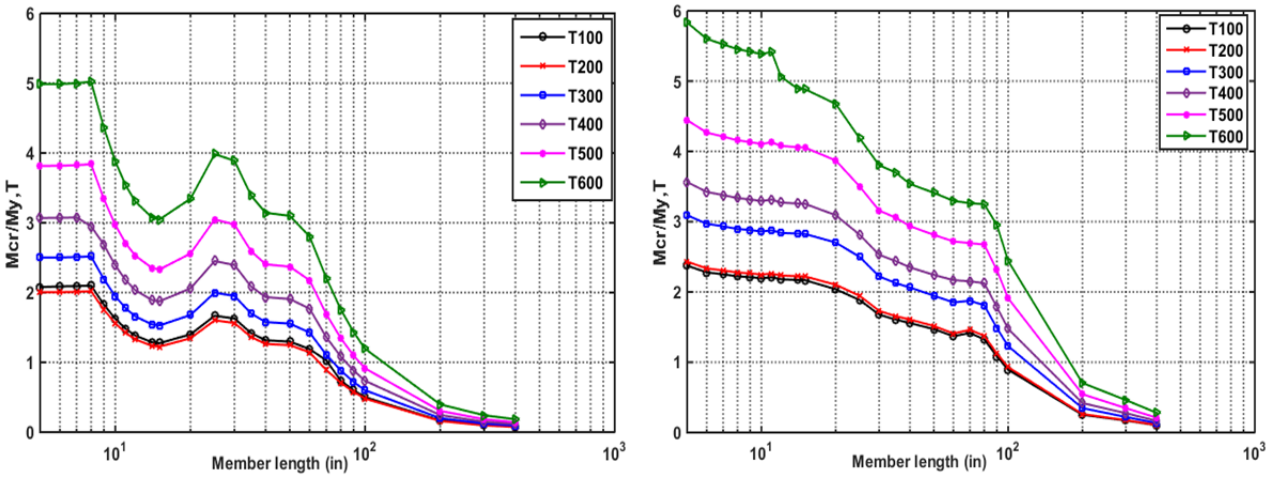

(a) (b)

Fig. 4 Normalized critical buckling moment for section 362S200-54 (a) uniform and (b) non-uniform.

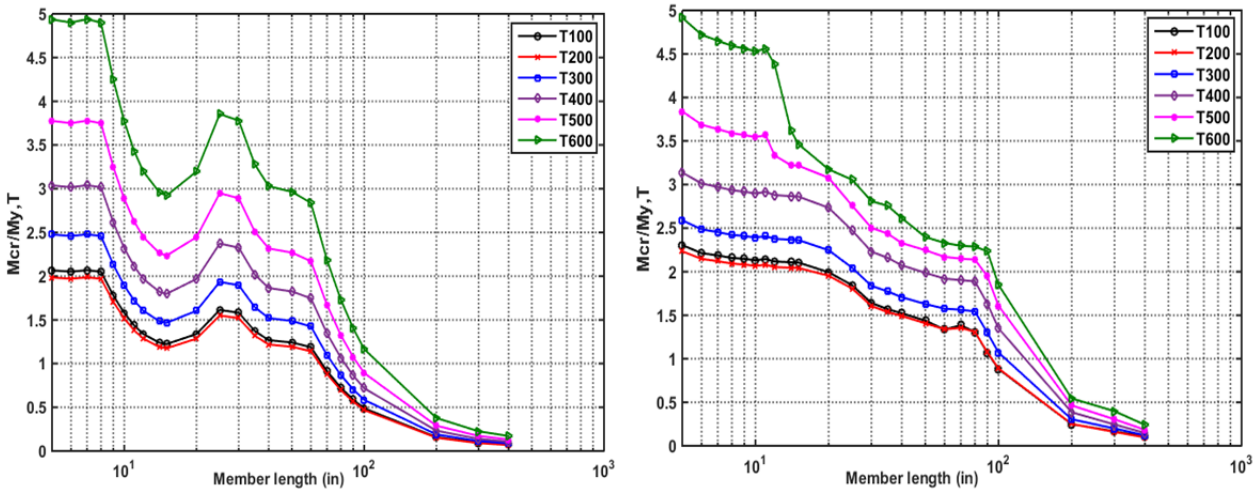

(a) (b)

Fig. 5 Normalized critical buckling moment for section 400S200-54 (a) uniform and (b) non-uniform.

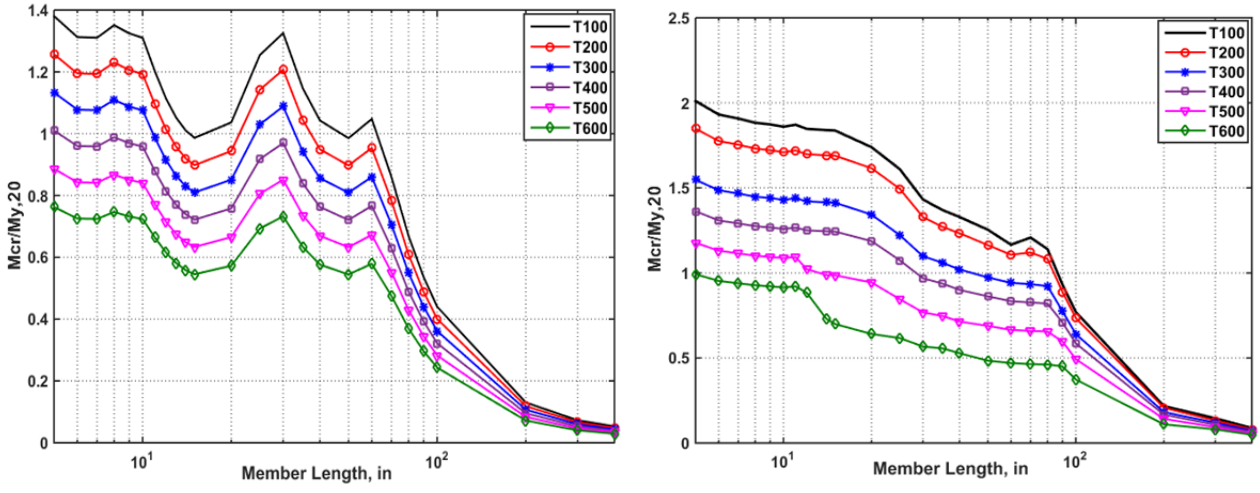

(a) (b)

Fig. 6 Normalized critical buckling moment for section 600S200-54 (a) uniform and (b) non-uniform.

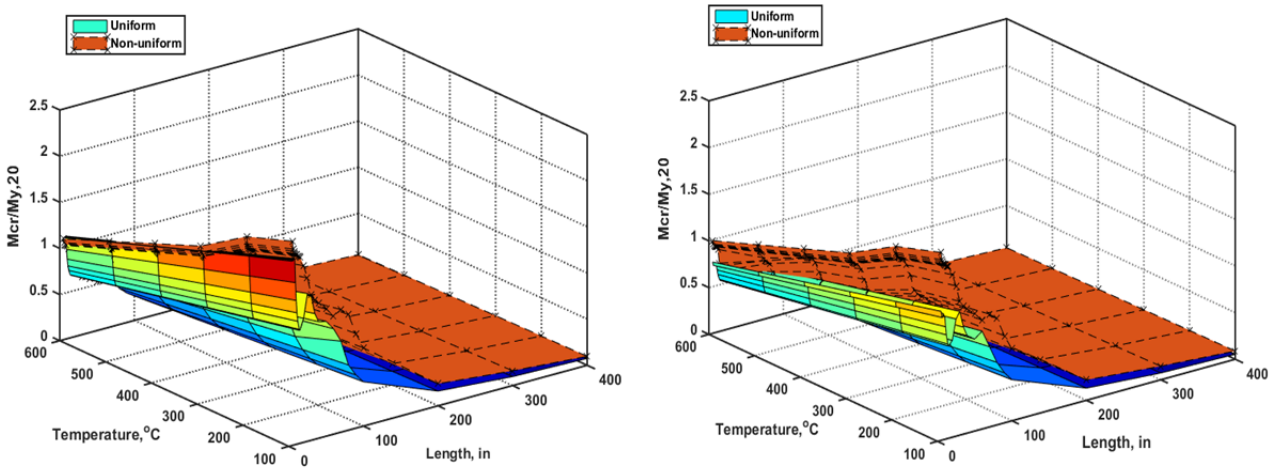

Fig. 7 Critical moment comparison under uniform and non-uniform temperature distribution for section (a) 362S200-54 and (b) 600S200-54.

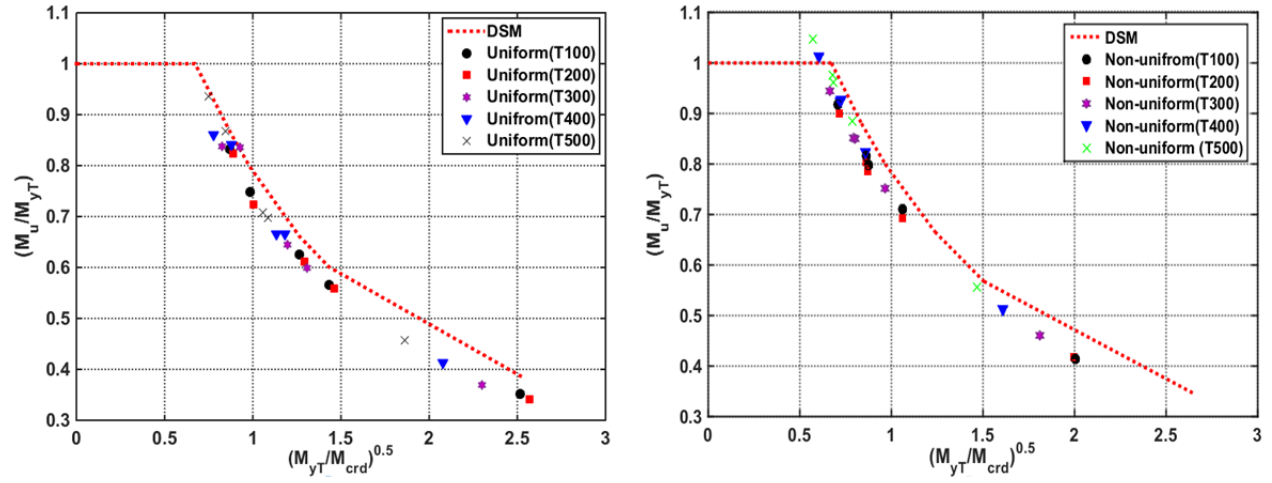

Fig. 8 Moment capacity prediction of section (a) 362S200-54 and (b) 600S200-54 under non-uniform elevated temperature.

4.2 Collapse Behaviour of CFS Beams under Non-uniform Temperature Distribution

The results obtained from elastic buckling analysis mostly predicted a higher critical buckling moment than the actual resisting capacity of the sections. This is true as the material property in such analysis uses the entirely elastic property, even if the material reaches its yield point. Thus, to observe the true buckling behavior, the material property has to be modeled with its yield stress specified during the analysis using an appropriate temperature-dependent stress-strain model. There are two ways to model material properties. One is the elastic-perfect plastic-type which assumes the yield stress on the material remains unchanged with an increase in plastic strain while the second modeling is an isotropic strain hardening, which allows the stress to increase with the plastic strain. Based on the experimental result by Kankanamge [2], higher grade CFS shows isotropic hardening behavior at both ambient and elevated temperatures whereas, low-grade CFS shows a well-defined yield point at a temperature range below 500 °C. The stress-strain model at the elevated temperature used was based on the Ramberg-Osgood stress-strain model modified by Kankanamge and

Mahendran [17]. The non-linear buckling analysis was then performed using the RIKS ON algorithm which provided LPF (load proportionality factor) versus Arch length. The predefined non-uniform temperature distribution was first imported from the heat transfer output files and the first Eigen-moment from the elastic analysis was then applied at the simply supported end for each time step. This operation is repeated for all sections. The finite element (FE) simulation moment capacity was then validated with the Direct Strength Method developed by Schafer [18].

Fig. 8 shows that the FE collapse analyses using uniform temperature distribution and direct strength method (DSM) for distortional section capacity are in good agreement for all temperature ranges considered in the collapse analysis. Up to 6.5% difference is observed for beam length 200 inches at a temperature of 400 °C. This difference is caused due to a combination of distortional buckling and lateral distortional buckling modes at such beam length. In all the temperature ranges, the DSM equation gives lower (conservative) section capacity than the FE collapse analysis especially for beam slenderness value ranging from 1 to 2.5.

5. Conclusions

This paper presented the results of a numerical simulation of the influence of uniform and non-uniform temperature distributions on the stability and moment capacity of the CFS channel beam section under pure bending and elevated temperature for three CFS channel sections. The following conclusions may be drawn:

- Non-uniform temperature distributions on the CFS channel beam resulted in a higher critical buckling and strength compared to uniform temperature distributions.
- Increasing the CFS section thickness and flange widths resulted in higher critical buckling moments for each temperature distribution.
- The critical moment for all the three sections exhibits mainly two buckling modes for all temperature ranges depending on member lengths. These buckling modes are local buckling and distortional.
- Even though the DSM equation for distortional buckling mode resulted in conservative section capacity, it can still be used without modification for uniform temperature distribution but might need further study to modify for the non-uniform temperature distribution cases.

Acknowledgments

The authors received no financial support for the research, authorship, and/or publication of this article.

References

[1] Keerthan, P., and Mahendran, M. 2012. "Numerical Modelling of Load Bearing LFS Walls under Fire Conditions." In *Proceedings of 7th International Conference on Structures in Fire.*

[2] Kankanamge, N. D. 2010. "Structural Behaviour and Design of Cold-Formed Steel under Elevated Temperatures." Ph.D. thesis, Queensland University of Technology.

[3] Cheng, S., Li, L. Y., and Kim, B. 2015. "Buckling Analysis of Cold-Formed Steel Channel-Section Beams at Elevated Temperatures." *Journal of Constructional Steel Research* 104: 74-80.

[4] Alfawakhiri, F. 2002. "Behaviour of Cold-Formed-Steel-Framed Walls and Floors in Standard Fire Resistance Tests." Ph.D. thesis, Carleton University.

[5] Shahbazian, A., and Wang, Y. C. 2011. "Calculating the Global Buckling Resistance of Thin-Walled Steel Members with Uniform and Non-uniform Elevated Temperatures under Axial Compression." *Thin-Walled Structures* 49 (11): 1415-28.

[6] Yin, Y. Z., and Wang, Y. C. 2003. "Numerical Simulations of the Effects of Non-uniform Temperature Distributions on Lateral Torsional Buckling Resistance of Steel I-Beams." *Journal of Constructional Steel Research* 59 (8): 1009-33.

[7] Alfawakhiri, F., and Sultan, M. A. 2000. "Fire Resistance of Loadbearing LSF Assemblies." In *Proceedings of the 15th International Specialty Conference on Cold-Formed Steel Structures*, St. Louis, MO, U.S.A.

[8] Sultan, M. A., Alfawakhiri, F., and Bénichou, N. 2001. "A Model for Predicting Heat Transfer through Insulated

Steel-Stud Wall Assemblies Exposed to Fire." In *Proceedings of Fire and Materials 2001 International Conference*, San Francisco, CA, U.S.A.

[9] Kontogeorgos, D., Wakili, K. G., Hugi, E., and Founti, M. 2012. "Heat and Moisture Transfer through a Steel Stud Gypsum Board Assembly Exposed to Fire." *Construction and Building Materials* 26: 746-54.

[10] Kukuck, S. 2009. *Heat and Mass Transfer through Gypsum Partitions Subjected to Fire Exposures*. Building and Fire Research Laboratory, National Institute of Standards and Technology.

[11] Ali, E. Y., and Bayleyegn, Y. S. 2018. "Application of the Direct Strength Method to Functionally-Graded-Material-Sheathed Cold-Formed Steel Beam Channel Members under Non-uniform Elevated Temperature." In *Proceedings of the Annual Stability Conference*, Baltimore, Maryland: AISC.

[12] Ali, E. Y., and Bayleyegn, Y. S. 2019. "Analytical and Numerical Buckling Analysis of Rectangular Functionally-Graded Plates under Uniaxial Compression." In *Proceedings of the Annual Stability Conference*, St. Louis, Missouri, AISC.

[13] Feng, M., Wang, Y. C., and Davies, J. M. 2003. "Thermal Performance of Cold-Formed Thin-Walled Steel Panel Systems in Fire." *Fire Safety Journal* 38 (4): 365-94.

[14] Gerlich, J. T. 1996. "Design of Light Steel-Framed Walls for Fire Resistance." *Fire and Materials* 20: 79-96.

[15] Chen and Young, 2004. "Mechanical Properties of Cold-Formed Steel at Elevated Temperatures." In *Proceedings of the 17th International Specialty Conference on Cold-Formed Steel Structures*.

[16] Ranawaka, and Mahendran. 2009. "Experimental Study of the Mechanical Properties of Light Gauge Cold-Formed Steel at Elevated Temperatures." *Fire Safety Journal* 44: 219-29.

[17] Kankanamge, N. D., and Mahendran, M. 2011. "Mechanical Properties of Cold-Formed Steels at Elevated Temperatures." *Thin-Walled Structures* 49 (1): 26-44.

[18] Schafer, B. W. 2008. "Review: The Direct Strength Method of Cold-Formed Steel Member Design." *Journal of Constructional Steel Research* 64 (7-8): 766-78.

Journal of Civil Engineering and Architecture 15 (2021) 294-299
doi: 10.17265/1934-7359/2021.06.002

The Importance of Design Spectra and Site Class for the Design of High-Rise Buildings

Anjeza Gjini, Hektor Cullufi, Altin Bidaj and Enio Deneko
Faculty of Civil Engineering, Polytechnic University of Tirana, Tirana, Albania

Abstract: On November 26, 2019 a strong earthquake of magnitude M6.4 occurred close to the City of Durrës, Albania (15.6 km WSW (west southwest) of Mamurras and 22 km SSW (south southwest) of Durrës), causing fatalities and considerable damages in many buildings. In this article we present and analyze, by means of observational data and numerical simulation, the behavior under this earthquake of an 8-floor RC (reinforcement concrete) building, by using design spectra referring to KTP-N.2-89 and Eurocode 8. The main purpose of the authors is to better understand and evaluate the seismic performance of high-rise buildings under the design spectra with a period of soil oscillation close to the fundamental period of the structure.

Key words: 2019 earthquake Durrës, design spectra, site class, structural damage.

1. Introduction

Durrës is one of the oldest cities in Albania (known as "Dyrrahum"), with a history of over 2,500 years. The region of Durrës is subjected to several strong earthquakes (I0 > VIII EMS-98). The most significant earthquakes of the latest 30 years occurred in September and November 2019, with the later one being the most devastating in Durres region. The earthquake of November 26, 2019 was a 6.4 magnitude earthquake, about 16 km off the coast of Mamurras at 3.54 CET (Central European Time) [1]. The most affected area was Durrës and Thumanë, while significant damages were reported in Shijak, Kruja, Tirana, Kamza, Kavaja, Kurbin and Lezha, as well. The earthquake caused 51 fatalities, 913 people injured at least, and the damages of hundreds of buildings [2].

2. Geotechnical Context

The geological, engineering-geological, geophysical and geomorphological settings that characterize the subsoil of a country are important factors to analyze the earthquake-induced phenomena manifested during the seismic events. Durrës City is situated close to Adriatic Sea. The plain of Durrës City is composed by very thick poor Quaternary sediments, which reach more than 130 m below [3]. The central area of the town comprises of organic layers of the former Durrës swamp (Qh-Holocene. Swamp deposits: clays, silts, sands and peats) or alluvial and proluvial deposits (Qp-h-Pleistocene-Holocene: sands, gravels and silts). The south, along the bay, consists of marine deposits, mainly sandy soils, and in the east (inland) to alluvial deposits. In all Periadriatic area of Albania, the liquefaction phenomena are observed during the earthquakes. In Durrës the phenomena of fountains with hot water and sand can be mentioned, during the earthquake in December 27, 1926, with 6.0 Magnitude [4]. According to different studies, Durrës City has a high potential liquefaction assessment.

3. The November 26, 2019 Earthquake

The earthquake of 26 November 2019, 3.54 CET, hit the north-central Albania. Parametric data of the earthquake are determined from different agencies. According to the data obtained from USGS (United

Corresponding author: Anjeza Gjini, M.Sc., lecturer, research field: structural engineering.

States Geological Survey) Earthquake Hazards Program [1], the November 26, 2019 earthquake in Albania occurred as the result of thrust faulting near the convergent boundary of the Africa and Eurasia plates. This seismic activity had the following properties:

- Event time: 3.54 CET
- Event location: 15.6 km WSW of Mamurras, Albania
- Epicenter depth: 22 km
- Magnitude (ML/MW): 6.3/6.4

Fig. 1 shows the earthquake components on three axes and magnitude.

4. Structural Damages in 9-12-Storey Buildings with RC Frame System

After the year 2001, the number of high-rise buildings constructed in Durrës is increased rapidly. These buildings are designed mainly based on the Albanian Technical Codes KTP-N.2-89 (which includes the seismic design norms) [5], and on European norms (Eurocode), although until 2018, KTP-N.2-89 was the legal one. The main structure of these high-rise buildings is reinforcement concrete frame, with/without core wall and shear walls, and masonry infills, supported by raft foundation. The failure observed from Durrës Earthquake varied depending on the location, building type and the year of construction. The damages were evident in structural and non-structural elements. For this typology of buildings, most of the damages are evident in non-structural elements. From the empiric analyses of RC frame system, the fundamental period of these structures is greater than those referred in Eurocode. This leads to the reduction of seismic forces, but on the other hand produces large interstorey drift, which is reflected in the damages of non-structural elements (masonry infills), also in-plane and out-of-plane failures. Even for RC frame combined with core wall or shear walls, there are evident problems not related to damages of structural or non-structural elements, but due to the fundamental period of the structures, which approximates to the period of soil oscillation. The incorrect design of the foundation has led to the phenomena of inclination. The differential settlement of the foundation may be old in time, due to the irregularity in plan and height of the buildings, as well as the *P-Δ* effect. However, the determining factor of the inclination of some buildings (up to 3%) has been the seismic actions, produced especially by the November 26, 2019 Earthquake. From the inspection carried out of these high-rise buildings, by taking in consideration the requirements of EC-2, [6], the key factors of their damages can be listed:

- The design of these buildings as very elastic structure, placed in foundation with period of oscillation ranging 0.3-2.0 s (referring to the Seismological Report of soil in the “D.Peza” street, Durrës, author Prof. Dr. Llambro Duni, 02.07.2010);
- Differential settlement of the foundation due to the irregularity in plan and height, and seismic actions;
- Inadequate structural system. In most cases they are designed as 3D reinforcement concrete frames, not combined with core or shear walls. In addition, there is evidence of hidden beams in slabs, causing the reduction of stiffness of the structure;
- The design of the stairs is done incorrectly, by using beams that reduce the height of the columns, causing the “short-columns” effect;
- Inadequate design of foundation, missing piles, even when they are necessary for transmission of vertical forces and seismic action;
- In many cases, which are composed of several sections on the same foundation slab, or buildings that are close to each other, seismic joints (seismic separation) are incorrectly designed or missing, causing the effect of the collision.

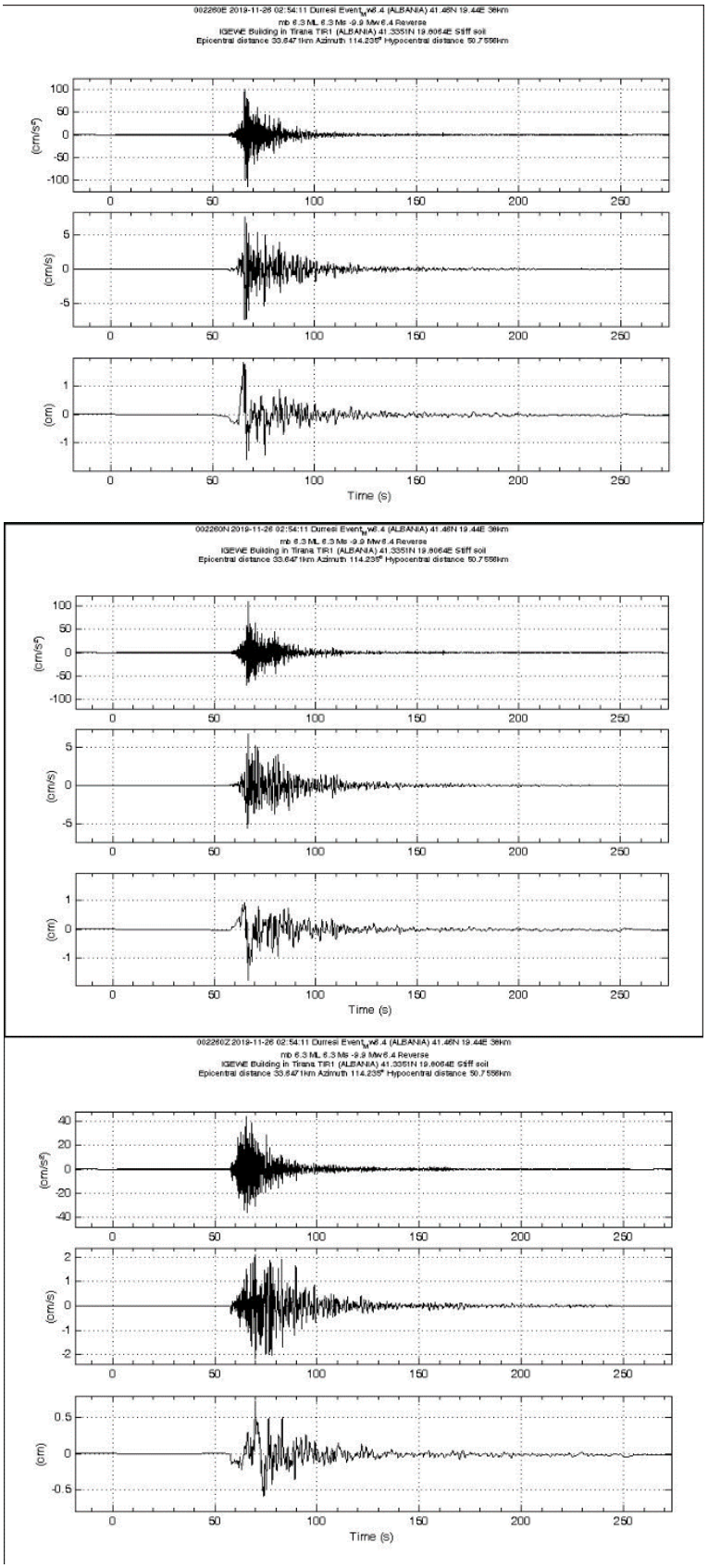

Fig. 1 November 26, 2019 earthquake, (a) E-W component, (b) N-S component, (c) Z-component [7].

5. Case Study

After the main shock of November 26, 2019 earthquake, many engineers from different countries (also from Italy, Republic of North Macedonia, Kosovo, Greece, etc.) and academic staff from the Faculty of Civil Engineering in Tirana organized a post-earthquake reconnaissance field mission. The scope was to observe structural and geotechnical damage patterns, evaluate the seismic performance of structures and explore the potential in code prevision for the design and retrofit of earthquake-resistant structures. During this mission, different areas in the Durrës region were inspected (as shown in Fig. 2). For the purpose of this study, the inspected buildings are 9-12-storey, located in the same geological conditions.

The studied 8-floor structure is a reinforcement concrete frame, composed by two rows of columns in a distance of 5.5 m in the transverse direction, and by five columns in a distance of 5.0 m in the longitudinal direction. The columns have a rectangular section of 120 × 40 cm along the verticality.

Beams along the perimeter are designed with rectangular section, and the other ones are concealed in reinforcement concrete slabs, so called "hidden beams" (h = 30 cm). The structure is designed with raft foundation (h = 110 cm), supported by R/C piles with a diameter of 50 cm and 650 cm long. The structure has no irregularity in plan and height.

The structure is modelled using advanced software such as ETABS Ultimate 19 (Fig. 3). This mathematical model can capture a satisfying degree of all actions on structure exerted by self-weight, imposed loads, seismic events and the effects of their combinations. For the purpose of this study, zero displacement is assumed for the vertical elements in the fixed support. The study is done according to KTP-N.2-89, Eurocode 8 [8] for T_c = 0.8 s (soil type D), and for T_c = 1.0 s that best suits seismic microzoning. The maximum displacements related to elasto-plastic stage is analyzed, that will be the elastic displacement amplified by the coefficient "q". The studied structure lies on soil that has a fundamental period T_p = 1.72 s, according to seismic report. The same interstorey mass is accepted referring to the Eurocode and Albanian Technical Code in the calculation of vertical loads that affect the seismic action, regardless of the differences between them According to the seismic report, the most suitable design spectrum is the one with period T_c = 1.0 s.

Fig. 2 Inspected area in Durrës.

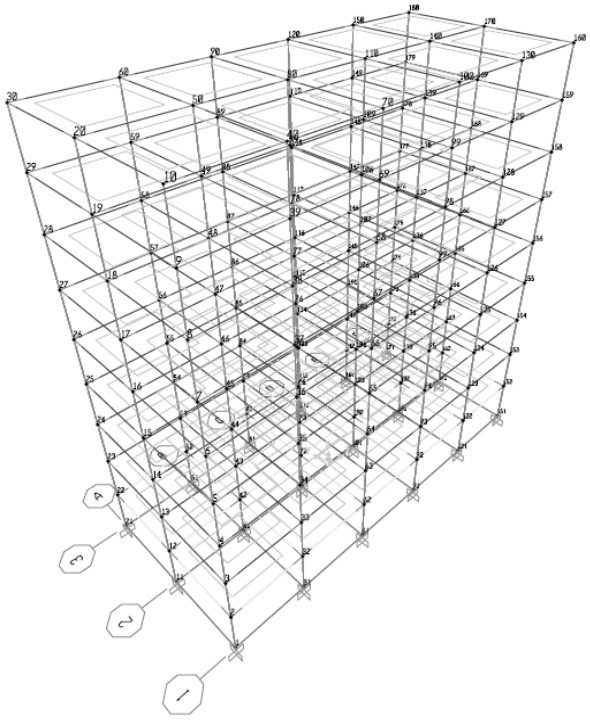

Fig. 3 Building with RC frame, 8-floor.

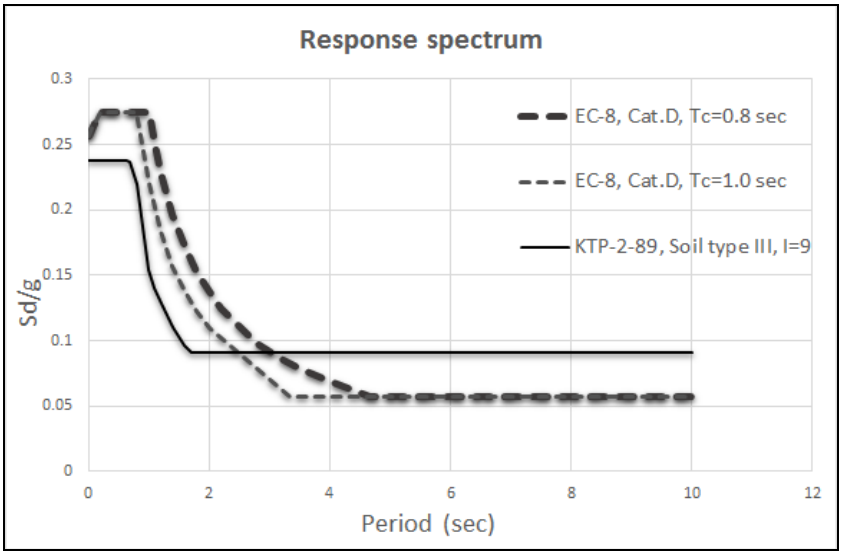

Fig. 4 Response spectrum according EC-8 (for T_c = 0.8 s and T_c = 1 s) and KTP-2-89 [5, 8].

Table 1 Base reaction.

S_D/g	F_X (kN)	F_Y (kN)	F_Z (kN)	M_X (kN-m)	M_Y (kN-m)	M_Z (kN-m)
RS1	1,340.04	4,458.53	0.0032	83,090.4	23,820.8	1.06
RS2	1,636.34	5,447.72	0.00328	103,837.7	29,762.4	1.06
RS3	1,076.52	3,218.32	0.00278	58,115.3	18,914.8	0.92

Table 2 Elastic Joint displacement.

S_D/g	*U*1 (cm)	*U*2 (cm)	*U*3 (cm)	*R*1 (Rad)	*R*2 (Rad)	*R*3 (Rad)
RS1	4.574	11.707	0.139	0.004	0.000	0.000
RS2	5.710	14.629	0.173	0.004	0.001	0.000
RS3	3.634	8.190	0.099	0.003	0.000	0.000

Table 4 Drift control for both directions.

Level	Interstorey drifts					
	Direction U1			Direction U2		
	RS1	RS2	RS3	RS1	RS2	RS3
R	0.001	0.001	0.001	0.006	0.008	0.005
8	0.002	0.002	0.001	0.007	0.009	0.005
7	0.003	0.003	0.002	0.009	0.011	0.006
6	0.003	0.004	0.003	0.010	0.012	0.007
5	0.004	0.005	0.003	0.010	0.013	0.007
4	0.004	0.005	0.003	0.010	0.012	0.007
3	0.005	0.006	0.004	0.009	0.011	0.006
2	0.003	0.004	0.003	0.006	0.007	0.004
1	0.002	0.002	0.001	0.002	0.003	0.001
0	0.000	0.000	0.000	0.000	0.000	0.000

6. Results

In Fig. 4 are shown the design spectra according to KTP-N.2-89 and EC-8 for different periods. From the analysis of the structure, the results present the effect of design spectra on the maximum displacements of the structure and the base reactions.

Fig. 5 Damages of non-structural elements.

As shown in Table 1, by using response spectra RS2, the base reactions increase by 22.1% (RS1) and 52% (RS3) for "*F*x", whereas for reaction in the other direction specifically 22.1% (RS1) and 69.2% (RS3).

According the results in Table 2, by using response spectra RS2, the maximum displacement increases by 24.8% (RS1) and 36.3% (RS3) for U1, and for displacement in the other direction specifically 24.9% (RS1) and 78.6% (RS3).

Table 3 shows the results from the model for the control of interstorey drifts in both directions (U1 and U2). Using response spectra RS2 (EC-08, for T_c = 1.0 s, soil type D) the minimum condition for interstorey drifts according to EC-8, for direction U2 is not satisfied.

Due to larger interstorey drifts, the building suffered damages of non-structural elements (masonry infill) and in-plane and out-of-plane failures, as shown in Fig. 5.

7. Conclusions and Recommendations

The analyses of this study conclude that it is important to choose the correct design spectra for structures built on land (soil) with periods close to that of the structure. Thus, the illusion can be avoided that by designing according to the spectra given by the technical codes we achieve the no-collapse requirement of the building. This condition relates to the fact that the structure does not suffer either local or global collapse. For structures with a height of 8-12 floors, which have the greatest damage mainly in the failure of the filling walls and inclinations in some cases, using a response spectrum according to EC-8, by accepting Tc = 1.0 s, leads to an increase of max displacements up to 24% and base shear force up to 22.1%. All these reflect in the incorrect reduction of the design parameters for the structure and its design (dimensioning and reinforcement) with lower values than required.

An important conclusion is the avoidance of high-rise buildings (especially in the range of 8-14 floors) in the areas where the period of soil oscillations is in resonance with the fundamental period of the structure.

References

[1] Earthquake Hazards Program. Accessed 30 November 2019. https://earthquake.usgs.gov/.

[2] Republic of Albania, Council of Ministers. 2020. *Albania Post-Disaster Needs Assessment Report*.

[3] Kociu, S. 2004. "Induced Seismic Impacts Observed in Coastal Area of Albania: Case Studies." In *Proceedings of the Fifth International Conference on Case Histories in Geotechnical Engineering*.

[4] Aliaj, S., Kociu, S., Muco, B., and Sulstarova, E. 2010. *Seismicity, Seismotectonics and Seismic Hazard Assessment in Albania.* Tirana: The Academy of Sciences of Albania.

[5] Akademia e Shkencave, Ministria e Ndertimit. 1989. *Kusht Teknik i Projektimit per Ndertimet Antisizmike, KTP-N.2-89*, Albania. (in Albanian)

[6] CEN. 2003. "Part 1-1: General rules and rules for buildings." In *EN 1992-1. Eurocode 2: Design of Concrete Structures.*

[7] Institute of Geosciences, Energy, Water and Environment in Albania. https://www.geo.edu.al/tirana_record/.

[8] CEN. 2004. "Part 1: General Rules, Seismic Actions and Rules for Buildings." In *EN 1998-1. Eurocode 8: Design of Structures for Earthquake Resistance*.

Journal of Civil Engineering and Architecture 15 (2021) 300-317
doi: 10.17265/1934-7359/2021.06.003

Performance Assessment of the Overall Building Envelope Thermal Performance—Building Envelope Performance (BEP) Metric

Simon Pallin[1], Carl-Eric Hagentoft[2], Antonio J. Aldykiewicz, Jr.[1], Jason W. DeGraw[1] and Mahabir Bhandari[1]

1. Building Envelope & Urban Systems Research Group, Oak Ridge National Laboratory, Energy and Transportation Division, 1 Bethel Valley Rd, Oak Ridge, TN 37830, USA

2. Department of Architecture and Civil Engineering, Division of Building Technology, Chalmers University of Technology, Chalmersplatsen 4, Gothenburg 41296, Sweden

Abstract: Today, to describe the thermal performance of the building envelope and its components we use a variation of metrics; such as, *R*-value, ACH (air exchange rate per hour), SHGC (solar heat gain coefficient) of windows, U-factor etc. None of these performance indicators is meant to represent the overall thermal performance. In this paper, such a metric is introduced, the BEP (building envelope performance) value. Unlike the thermal resistance, typically expressed as an *R*-value, the BEP-value considers additional elements of heat transfer that affect the energy demand of the building because of exterior and interior (solar) thermal loads: conductive and radiant heat transfer, and air infiltration. To demonstrate BEP's utility, validation studies were carried out by comparing the BEP-value to theoretical results using whole building energy simulation tools such as EnergyPlus and WUFI Plus. Results show that BEP calculations are comparable to calculations made using these simulation tools and that unlike other similar metrics, the BEP-value accounts for all heat transfer mechanisms that are relevant for the overall energy performance of the building envelope. The BEP-value thus allows comparing envelopes of buildings with different use types in a fair and realistic manner.

Key words: Building enclosure, energy, *R*-value, EUI (energy use intensity), airtightness, building envelope campaign.

Nomenclature

a	Thermal diffusivity (m^2/s)
A	Surface area (m^2)
b	Thermal effusivity ($(W\cdot\sqrt{s})/(m^2\cdot K)$)
BEP	Building envelope performance ($J/m^2\cdot year$)
C_{air}	Specific heat of air ($J/(kg\cdot K)$)
C	Air flow coefficient
cM	Interior thermal mass (J/K)
d	Equivalent thickness (m)
I_{sol}	Incident solar heat load (W/m^2)
K	Thermal conductance (W/K)
L	Material thickness (m)
M	Air infiltration rate (m^3/s)
q	Heat flux (W/m^2)
Q	Thermal load or heat flow rate (W)
R	Thermal resistance, *R*-value ($(m^2\cdot K)/W$)
R_{se}	Overall exterior surface heat transfer resistance ($(m^2\cdot K)/W$)
$R_{se,c}$	Convective exterior surface heat transfer resistance ($(m^2\cdot K)/W$)
$R_{se,r}$	Radiant exterior surface heat transfer resistance ($(m^2\cdot K)/W$)
R	Whole-Building thermal resistance ($(m^2\cdot K)/W$)
t	Time (s)
T	Temperature (K)
U	Thermal transmittance, *R*-value ($W/(m^2\cdot K)$)
α	Material solar absorptivity (-)
ε	Material infrared emissivity (-)
σ	Opaque envelope solar and thermal radiation correction factor (-)
ρ_{air}	Density of air (kg/m^3)

Corresponding author: Simon Pallin, PhD, research fields: heat and mass transfer in buildings and systems.

1. Introduction

In many cases, engineers, architects, consultants and building owners use prescriptive measures to quantify the thermal performance of the building enclosure. For example, steady state measurements such as material *R*-values or U-values are used to calculate the composite thermal resistance or

transmittance of the building envelope. These values are then used to determine the overall thermal performance of the building envelope in the absence of dynamic effects. Unfortunately, it is well known that *R*-value alone does not account for the building envelopes response to energy transfer [1]. Other factors, such as thermal mass, the thermal properties of fenestrations, air infiltration, occupant behavior and climate, especially solar loads, all play a role in determining the overall performance of the building envelope. It is these properties and the relationships between them that make quantifying or developing a metric, a more representative metric, of the building envelope's thermal performance complicated. For example, whole building energy simulations account for these properties separately rather than use a single metric to account for the thermal performance of the building envelope The final result of the energy simulation is often used to compute metrics that describe the performance of the building as a whole, including HVAC (heating, ventilating and air conditioning) system, plug loads, lighting, etc. One such metric is the EUI (energy use intensity), which is the energy use of the building per conditioned floor unit area. The properties and performance of the building envelope, good or bad, are just one part of these results.

While quite a bit of effort has been focused on trying to capture or develop a measure of the building envelope's thermal performance that is more representative of the dynamic behavior, these efforts are complicated by three dimensionality: heterogenous properties, and dependence on climate [2]. Nevertheless, the importance of the envelope has inspired numerous efforts over the years to find better measures.

The M-factor is one such measure that tried to explain the effect of thermal mass on the performance of the building envelope that was not reflected in or accounted for by the steady state *R* value. [2]. The M-factor was defined as the ratio of the dynamic heat flux of the masonry wall to theoretical steady state values. That value was then used as a correction factor to the steady state conduction equation to account for thermal mass. When the heat flux was measured over a short period of time, approximately 1 h, there was a difference or a dependence on thermal mass [3]. However, Godfrey et al. [3] showed that when measurements were made over a longer period (e.g. a day or more), the net heat flux was independent of thermal mass. Godfrey et al. [3] concluded that to attribute the effect of thermal mass to walls alone was incorrect and that other factors were needed to be considered. These factors include solar loads, internal loads and the transient response to meet the energy demands required to maintain thermal comfort. They correctly pointed out that all these variables and their interrelationship need to be considered to accurately account for the thermal performance of the building enclosure.

Later, Kosny et al. [4] introduced a new measure, the DBMS (dynamic benefit for massive systems), to account for the effect of thermal mass on the performance of the building envelope. This approach took into consideration the materials that comprised the building envelope and its configuration while also accounting for climate. The approach was based on the determination of an equivalent *R* value for massive walls with the same heating and cooling requirements as a wood framed wall exposed to the same climate. The ratio of the two was defined as the DBMS. Kosny et al. [4] showed that thermal mass does play a role and depends on both the configuration of the wall and exterior climate. In hot climates, the effect is greater compared to cold climates. Results also showed that the greatest benefit was associated with constructions where the massive elements were proximate to the interior side of the building envelope. The approach was primarily used to study the effect of thermal mass on the building envelope.

The same approach would later be used to quantify the benefits of green roof systems [5]. Moody and

Sailor [5] showed that for the case of green roofs, when evaporative cooling is active as a result of the soil's moisture content, the green roof increases heating loads resulting in a higher energy demand. Defining the metric as DBGR (dynamic benefit of green roofs) they were able to show the dependence of climate zone on the utility of green roofs relative to conventional roofs with equivalent steady state *R* values. The DBGR is defined as the ratio of the HVAC loads between a building with a conventional roof system and one that is comprised of a green roof. A value of one means there is no benefit. A value greater than one means that the green roof is more energy efficient or results in lower HVAC loads compared to the conventional building or roof. A value less than one means that the conventional roof has lower HVAC loads relative to a green roof. More importantly, they were able to validate the metric using real moisture dependent material properties and weather data. The standard deviation between the simulations carried out using EnergyPlus [6] and experimental results were between 1.5 °C and 4 °C for the winter and summer months, respectively.

In an effort to better understand the impact of air exchange on the thermal performance of residential buildings the Incremental Ventilation Energy (IVE) model was developed [7]. The issue with the energy consumption in the residential housing stock is large scale air changes. These air changes result in a significant increase in energy demand. The problem with current energy models is that many of the physical processes such as heat transfer across the building envelope are not affected by air changes. To account for that change, the model accounts for the change in energy demand as a result of air change. Coupled with a set of housing characteristics, the model can then be used to predict the impact on energy demand as a result of reducing air leakage across the building envelope. Though, the air change model or IVE is physics based, the calculation of total energy demand is based on a population of homes and their characteristics. There are some other limitations associated with infiltration. For example, the model considers all infiltration and ventilation coming from outside the building envelope. It does not account for air change between conditioned and unconditioned spaces. These are just some of the limitations. However, as a comparative tool, it does meet the technical objective of trying to understand the impact of air change reduction on the energy demand of a population of residential homes.

Alterman et al. [8] took a different approach to try and develop a holistic measure of the BEP. In studying the effect of thermal mass on the performance of the building's energy demands, field measurements showed that similar internal conditions could be obtained for walls with significantly different steady state *R*-values. This led to the development of an approach to quantify or capture all the effects or properties of the wall including the effect of climate in one value defined as the dynamic temperature response or *T* value. The *T* value is a function of the dynamic profiles of the exterior climate and the response of the building's internal temperature. The relationship between the two results in an ellipse with a characteristic inclination angle defined as the dynamic temperature response. For example, if the wall behaves as an insulator the inclination angle is 0°. For a perfect conductor, the inclination angle is 45°. Using this approach, they were able to differentiate between massive and light framed constructions by measuring the differences in the inclination angle coupled with the principal components of the dynamic temperature profiles.

Building on the work of Alterman et al. [8], Arkar and Perino [9] developed a metric based on the *T* value to account for the dynamic response of what they refer to as adaptive materials in the building envelope such as phase change materials. Instead of measuring the dynamic temperature profiles, they used the envelope's inner surface heat flux. The sol-air temperature was selected as the exterior boundary

condition. The new measure, *U* dynamic thermal performance metric, was calculated using a linear fit to the daily thermal response through the origin. The *T* metric effectively captured the effect of thermal inertia. In theory, the metric could be used to replace the U value in the calculation of envelope transmittance. More work needs to be done to determine its relationship to the static U value and the relationship to the overall BEP (building envelope performance).

To more accurately quantify the thermal performance of the building envelope Reilly and Kinnane [10] tried to separate out the effect of thermal mass in energy simulations by taking the ratio of the energy demand in a dynamic model to that calculated using a quasi-static model. They defined that measure as the TER (transient energy ratio). The TER was used to show the effect of wall materials, configuration and climate on the thermal performance of the building envelope. Results were consistent with the work of Kosny et al. [4]. BEP improved when massive elements were proximate to the interior and when the walls were exposed to hot climates. In cold climates, thermally massive walls resulted in increased heating loads compared to light framed walls.

It is worth noting that in 1975 American Society of Heating, Refrigerating and Air-Conditioning Engineers (ASHRAE) developed an approach to quantify the thermal performance of the building envelope in air-conditioned buildings by introducing the concept of OTTV (overall thermal transfer value) [11]. OTTV is defined as the maximum thermal transfer permissible in the building through its walls or roof due to solar heat gain and outdoor-indoor temperature differences. Unlike *R* or U value, the OTTV is a function of the thermal transmittance of the opaque and transparent portions of the building envelope, solar gains through windows, exterior and interior climate. OTTV has been adopted in the building codes in several ASEAN (Association of Southeast Asian Nations) countries with modifications throughout the years [12]. Hong Kong and Singapore have implemented a variation of its original form into sustainable building codes and building certifications [13]. ASHRAE abandoned the approach because of its limitation as a measure to account for internal loads [14]. Rather than continue to refine the metric, in a subsequent revision of the standard 90.1, ASHRAE decided to treat the impact of each of the properties separately through the implementation of whole building energy calculations with additional properties such as thermal inertia and air infiltration in the revision ASHRAE 90.1-1989 [15].

A significant challenge towards developing a single metric for the performance of the building envelope is to account for the effect of solar loads on surface temperatures, in particular, the impact it has on exterior building envelope surface temperatures and how that influences interior heat loads. One approach is to use the sol-air temperature [16] which defines a fictious ambient temperature that accounts for solar induced heat transfer through the opaque building envelope but does not reflect on solar induced interior heat gains.

There also exist various simplified methods to calculate heating and cooling loads from estimating the overall thermal performance of buildings, such as CLTD/CLF/SCL (cooling load temperature difference/cooling load factor/solar cooling load factor) [17] and the RTS (radiant time series) method [18]. Historically, both methods have been used as a simplified means to estimate cooling loads for the purpose of sizing HVAC equipment. As a result, they include all variables relevant to the energy demand in buildings including interior loads from solar radiation through windows. However, these methodologies do not generate a metric or single indicator that represents the BEP.

To facilitate comparison of similar building types, Wang and coworkers [19] developed a simple scoring system based on the distribution of EUI, the building energy asset score. Unlike some of the earlier approaches, the building energy asset score is a

measure of relative performance. In addition, the score is based on whole building energy simulations that accounts for mechanical, electrical, and service hot water systems. The building asset score is then used to identify parts or systems of the building where there are opportunities for energy reduction.

To balance the needs for accuracy and speed an RC (resistors and capacitors) network was developed to simulate the energy performance of the building [20]. The network takes into account heat transfer through the building envelope including the roof, and accounts for solar loads and the effect of building occupants and equipment. In simple terms, the resistive components represent heat transfer via conduction and convection while the capacitive terms account for the effect of thermal mass. A network is then developed based on sub-categories of building elements, e.g., walls, roofs, partitions and equipment. Depending on the net floor area and the peak power demand the order of the network is established and validated. Preliminary results indicate good agreement between measured and simulated net hourly heating demand. The challenge with this approach is keeping the network simple by minimizing the number of sub-categories and the network order. As the structure becomes more complicated, the benefits of the RC network may be lost. In addition, if there is a change in the peak energy demand as result of a structural or systems change, e.g., retrofit, the RC circuit and network order may have to be modified to account for the change in thermal performance making it a challenge to use as a comparative tool.

ISO 13789 [21] specifies a method and metric to account for whole building loads as is the focus of this paper. However, this standardized approach is based on steady-state calculation and thus will not account for any thermal inertia as associated with the building envelope and thermal mass of a building's interior.

This paper describes, in detail, the approach and development of the BEP-value that captures the thermal performance of the building envelope.

2. Method

This paper presents a simplified method to evaluate and investigate the proposed BEP-value as a metric of an overall building envelope thermal performance. Though a simplified method is used in this paper, any whole-building energy assessment simulation tool can be utilized to calculate the BEP-value if following the method as described in this paper.

In principle, a heat and energy balance of a building can be described in Eq. (1).

$$\begin{aligned} Q_{HVAC} &= Q_{env} + Q_{in} \\ Q_{env} &= Q_{cond} + Q_{env,air} + Q_{gain,sol} - C\frac{dT}{dt} \\ C &= \sum_i c_i \cdot M_i \end{aligned} \quad (1)$$

Whatever acts as a load on the HVAC system, Q_{HVAC}, is basically a result of two variables; the heat loss or gains through the building envelope components including any solar induced load, Q_{env}, and the heat loads generated inside the building, Q_{in}. In Eq. (1), C represents the sum of thermal mass from interior. The thermal mass of the building envelope is embedded in conductive heat transfer load, Q_{cond}.

The proposed metric accounts for interior loads due to solar loads, but not loads from lighting, plug loads and building occupants. The main reason for this is that the BEP-value represents the overall thermal performance of the building envelope and should not reflect on loads which are dependent on usage. Thus, the metric is based on the following principle.

$$BEP = \frac{\sum_{t=1}^{8760} \left| Q_{env}(t) \right| dt}{A_{env}} \quad (2)$$

In Eq. (2), we introduce the BEP-value, which is the ratio of the total annual building envelope related energy demand over the building envelope area, A_{env}. The reason why the building envelope area is used, rather than the conditioned floor area (as for EUI), is because the BEP-value represents the overall unitary BEP, regardless of how much floor space it encloses. Section 2.1 describes the simplified method used

throughout this paper to evaluate the BEP-value, what it represents and its application.

2.1 Solution Technique—Transient Response and Lumped Analysis Models

The transient response and lumped analysis models of this section account for all heat transfer that is associated with the building envelope, solar loads, as well as the thermal mass of the building envelope and the building interior. The approach presented consists of three parts: one to account for heat transfer through the opaque building envelope and its thermal mass, one to also account for convective and radiant heat transfer, and lastly, to connect all building envelope heat transfer with the thermal inertia of the building interior.

2.1.1 Thermal Response and Lumped Analysis of Building Envelope Conductive Heat Transfer

The first part of the transient heat transfer approach of this paper consists of two solutions: a response solution and a lumped analysis model. The reason the two solutions are used together is because their accuracy varies as the heat flux approaches steady state. The response solution does a reasonable job predicting the heat flux for short times, while the lumped analysis is used to solve for longer times. The second solution typically does not handle "smaller" times well, thus the two solutions become complementary. For more information on what is summarized in this section, the reader is referred to previous work [22].

The response solution for the internal surface conductive heat flux in an arbitrary opaque building envelope component, c, with N materials, $qi_{n,c}$ is given by the following expression.

$$q_{in,c}(t) = \frac{\lambda_N}{d}\frac{b_1}{b_N}2^N\left\{\prod_{i=2}^{N}\frac{b_i}{b_{i-1}+b_i}\right\}e^{\frac{a_N t}{d^2}+\frac{\sqrt{a_N}}{d}\sum_{i=1}^{N}\frac{L_i}{\sqrt{a_i}}} \cdot \operatorname{erfc}\left(\frac{\sqrt{a_N t}}{d}+\sum_{i=1}^{N}\frac{L_i}{\sqrt{4a_i t}}\right) \quad \ldots. (3)$$

Here, N represents the number of materials in the multilayer composite, as well as the number of the innermost material. d is an equivalent thickness representing the inner surface resistance, R_s. b is the thermal effusivity, α the thermal diffusivity, and L the thickness of each material.

$$\frac{d}{\lambda_N} = R_s, \quad a_i = \frac{\lambda_i}{\rho_i \cdot c_i}, \quad b_i = \sqrt{\lambda_i \cdot \rho_i c_i} \qquad (4)$$

For the lumped analysis and second approach for longer times, which is basically equivalent to a finite difference solution, the following equation system must be solved,

$$\frac{d\mathbf{T}}{dt} = \mathbf{A}\mathbf{T} + \boldsymbol{b} \qquad (5)$$

Here, $\mathbf{T}$ is a vector with element j = 1…N, representing the center temperature of each layer j. The initial condition is zero for all the $\mathbf{T}$ vector elements. $\mathbf{A}$ is a tridiagonal matrix. Eq. (5) represents a system of ordinary differential equations. It can be solved by various techniques [23].

$\mathbf{A}$ gives the basis for the approximation, in which each element corresponds to the layers of the composite. The general solution for the lumped case has the following form [24],

$$\boldsymbol{T} = \boldsymbol{T}_s - \mathbf{V}\exp(\mathbf{D}t)\,\mathbf{V}^{-1}\boldsymbol{T}_s \qquad (6)$$

The elements in the $\mathbf{T_s}$ vector represent the steady state temperature of the problem in Eq. (5). The matrix $\mathbf{V}$ of $\mathbf{A}$ has the eigenvectors of column vectors. The matrix $\mathbf{D}$ has the corresponding eigen values as diagonal elements. The principal solution of Eq. (6) will be of the following type,

$$T_i = T_{s,i} + \sum_{j=1}^{N} c_{ij} \cdot e^{-t/t_{cj}} \quad t_{cj} = -\frac{1}{\mathbf{D}_{jj}} \qquad (7)$$

Here, the characteristic time, t_{cj}, is the inverse of the eigenvalue $\mathbf{D}_{jj}$ in negative form. The largest characteristic time value will determine the behavior under this condition. In accordance with this statement,

an approximate expression for the interior heat flux at large time values uses the two largest characteristic time values.

$$\begin{cases} \dfrac{q(t)}{U} = 1 - C_1 \cdot e^{-t/t_{c1}} - C_2 \cdot e^{-t/t_{c2}} \\ t_{c1}, t_{c2} = \max(t_{cj}) \end{cases} \tag{8}$$

Finally, the chosen breakpoint, γ, for which Eq. (8) is used over Eq. (3) is be determined under the following conditions,

$$\frac{q(t_\gamma)}{U} = \gamma = 1 - C_1 \cdot e^{-t_\gamma/t_{c1}} - C_2 \cdot e^{-t_\gamma/t_{c2}} \tag{9}$$

Here, $q(t_\gamma)$ represents the interior heat flux found in Eq. (3) at time t_γ. The breaking point is chosen as the time when the heat flux has reached a certain level of full implementation, i.e. steady state. Post the time of this breakpoint, the approximation for short time values becomes less accurate as time increases. Consequently, this breakpoint also represents a time for which the temperature step change has propagated to a certain depth through the composite. Previous study [22] showed that the value of γ should be in the range of 0.1 to 0.3. For this study, γ is to be 0.2.

2.1.2 Overall Building Envelope Heat Transfer

The total building envelope heat transfer is given by the conductive heat transfer as seen in Section 2.1.1, but also heat transfer from air infiltration and solar heat gains through fenestrations. The overall building envelope heat load becomes,

$$\begin{aligned} Q_{env} &= \sum_{x=c}^{X} q_{in,c} \cdot A_{env,c} \cdot \left(T_{surf,c} - T_{in}\right) + \ldots \\ &+ K_{air} \cdot \left(T_{out} - T_{in}\right) + Q_{gain,sol} - C\frac{dT}{dt} \end{aligned} \tag{10}$$

where X is the number of building envelope components, c.

In Eq. (10), T_{surf} represents the surface temperature for each building component and is calculated according to a general definition of a roof surface as presented in Fig. 1, in which Tr is the sky temperature.

Further, an effective thermal resistance due to air infiltration through the building envelope, R_{air}, can be found using the overall air flow rate through the building envelope, $\dot{M}_{air}$.

$$R_{air} = \frac{A_{env}}{\dot{M}_{air} \cdot \rho_{air} \cdot c_{air}} \tag{11}$$

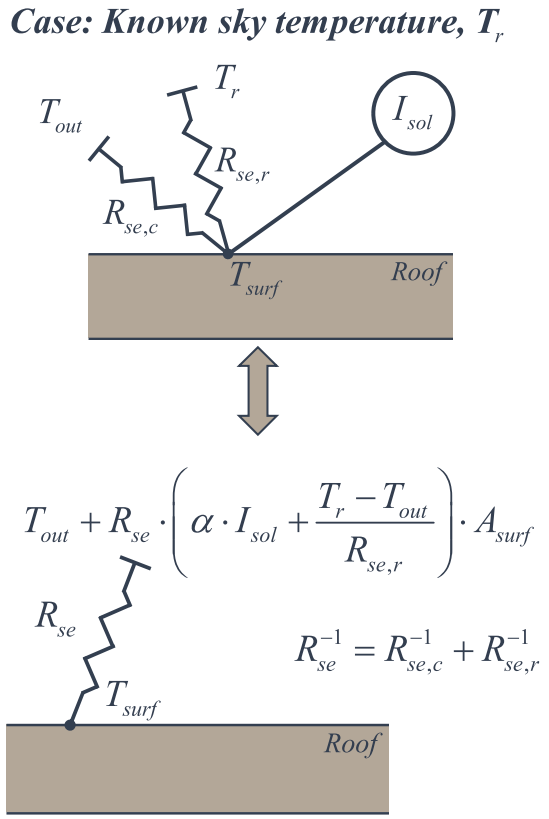

Fig. 1 Network reduction approaches to calculate equivalent roof surface temperature due to conductive, convective and radiant heat transfer.

In this study, a simplified approach is used to calculate the air flow rate, $\dot{M}_{air}$ [25]. Here, $\dot{M}_{air}$ is a function of the effective air leakage area, ELA and the air pressure gradient over the building envelope.

$$\dot{M}_{air} = ELA \cdot \sqrt{C_s \cdot \left|T_{out} - T_{in}\right| + C_w \cdot V_w} \tag{12}$$

in which, C_s and C_w are temperature boyancy and wind coefficients according to ASHRAE Fundamentals Chapter 16.10 [25]. Utilizing Eqs. (11)

and (12), the thermal resistance due to air infiltration is given by the following,

$$R_{air} = \frac{A_{env}}{ELA \cdot \sqrt{C_s \cdot |T_{out} - T_{in}| + C_w \cdot V_w} \cdot \rho_{air} \cdot c_{air}} \quad (13)$$

$$K_{air} = \frac{A_{env}}{R_{air}} \quad (14)$$

Consequently, K_{air} is the thermal conductance for air infiltration and natural ventilation.

Eq. (10) also includes $Q_{gain,sol}$, which is the interior thermal load from solar radiation through windows, and given by the product of the incident solar radiation load, I_{sol}, and the SHGC (solar heat gain coefficient).

$$Q_{gain,sol} = I_{sol} \cdot SHGC \quad (15)$$

For components without any notable thermal mass, such as windows, Eq. (3) is replaced with,

$$q_{in,c}(t) = U_c \quad (16)$$

Here, U_c is the U value of the building envelope component denoted by c.

2.1.3 Lumped Analysis of Building Envelope Heat Flux and Interior Mass

The inflow of heat from the building envelope, including air leakage and solar gains, will change the indoor temperature of a building. As a response to this change in temperature, the heating and cooling system will compensate for the same, and thus maintain the indoor temperature within user-defined thermal comfort boundaries. Thus, the building envelope related heat loads will act as a load on the HVAC system, Q_{env}.

A base heating and cooling load, Q^0_{env}, is introduced with an assumed fixed indoor temperature, $\overline{T}_i$, representing the average temperature inside the thermostat setpoint interval. To this process, a second temperature is given, T', representing that of the internal mass and superimposed,

$$\frac{Q_{env}(t) - Q^o_{env}(t)}{K_{env}} = t_c \frac{dT'}{dt}$$
$$t_c = \frac{cM}{K_{tot}} \quad K_{tot} = K_{env} + K_{air} \quad (17)$$

in which, cM (J/K[Btu/°F]) represents all interior thermal mass lumped together. The time scale, t_c, is determined by the ratio of cM and the total building thermal conductance between the interior and exterior, i.e. the denominator in Eq. (17), in which, K_{env}, represents the building envelope conductance for all building envelope components as,

$$K_{env} = \frac{\frac{A_{wall}}{R_{wall}} + \frac{A_{roof}}{R_{roof}} + \frac{A_{slab}}{R_{slab}} + U_{win} \cdot A_{win}}{A_{env}} \quad (18)$$

K_{air} is given by Eq. (14).

Importantly, the left term of Eq. (17) depicts the difference in energy load between a fixed and a varying indoor temperature (according to thermostat setpoints). This difference in energy is also the sum of energy absorbed/released by the internal mass within the temperature gradient, dT.

The building envelope heating and cooling load, Q_{env} in Eq. (10) is to be determined so that,

$$T_{\min} \le \overline{T}_i + T' \le T_{\max} \quad (19)$$

In the simulations of the interior temperature, for each hour of the year, the time constant is not changing its value, neither does the heat flow to the interior. Assuming a known interior temperature T_{n-1} at time t_{n-1} (i.e. n-1 hours into the calendar year), the first guess without applying any cooling or heating would be,

$$T'_{first\ guess}(t_n) = T'(t_{n-1}) + \left(\frac{-Q^o_{env}(t_n)}{K_n} - T'(t_{n-1}) \right) \cdot \left(1 - e^{-\Delta t / t_{c,n}} \right)$$
$$\Delta t = t_n - t_{n-1} \quad (20)$$

If the temperature is within the comfort span, the

temperature at time t_n is determined directly by Eq. (20). If not, heating or cooling is added to the heat flows in the expression so that the temperature remains equal to the set temperature span limit that has been passed:

$$\begin{aligned} &T'_{first\ guess}(t_n)+\overline{T}_i > T_{\max} \quad \Rightarrow \\ &T'(t_n)=T_{\max}, Q_{env}(t_n)= \\ &=-K\frac{T'_{first\ guess}(t_n)+\overline{T}_i-T_{\max}}{1-e^{-\Delta t/t_{c,n}}} \end{aligned} \tag{21}$$

or

$$\begin{aligned} &T'_{first\ guess}(t_n)+\overline{T}_i < T_{\min} \quad \Rightarrow \\ &T'(t_n)=T_{\min}, Q_{env}(t_n)= \\ &=-K\frac{T'_{first\ guess}(t_n)+\overline{T}_i-T_{\min}}{1-e^{-\Delta t/t_{c,n}}} \end{aligned} \tag{22}$$

2.2 Validation

The purpose of this study is mainly to introduce the BEP-value and portray what it represents in terms of overall building envelope energy performance. In order to do so, we have presented a simplified method.

For this validation, EnergyPlus and WUFI Plus [26] have been utilized. Since the proposed solutions in this study were developed in MATLAB®; various aspects of the generated simulation results require validation.

The incident direct and diffuse solar load utilized in the model is calculated using the horizontal infrared radiation intensity, direct normal solar radiation, and diffuse horizontal radiation given by EPW (EnergyPlus Weather) files, thus a validation is justified to ensure it matches input data generated by EnergyPlus.

Fig. 2 depicts the correlation between the solar radiation loads computed by EnergyPlus and the solar loads computed by the method developed under this study. Both EnergyPlus and simplified method utilize the Perez model [27] to estimate the diffusive solar load. Though there are some discrepancies, they are not significant enough to import weather data generated by EnergyPlus for this study. For direct solar loads, the discrepancy in average solar loads overall surface is 0.4%, while for diffuse solar loads it is somewhat higher, varying between 1.4% and 6.8% overall surfaces. Since this study aims to look at the variation of the proposed BEP metric for various building types and climates, the methodology implemented from the Perez model is assumed satisfying.

For further validation, a medium office building was simulated in WUFI Plus in accordance with the DOE (Department of Energy) prototype buildings and ASHRAE Standard 90.1 [28, 29]. The building was simulated in the climate of Atlanta, GA, USA. The simulation results generated by WUFI Plus and the simplified method were compared for total heating and cooling demand as depicted in Fig. 3 and reveals that a good agreement with the calculated cooling and heating demand between the two simulation models.

Finally, the proposed BEP-value is compared between the simplified model and WUFI Plus. Using the same Medium Office building as previously described [28, 29], the BEP-value was calculated and compared between 15 climates in the U.S., representing climate zone 1A through 8A. In accordance with the prototype building settings, the thermostat setpoints for cooling and heating varies between 21.1 °C and 23.9 °C. The result of the comparison is presented in Fig. 4 and reveals a close agreement with the results of the comprehensive WUFI Plus model and the simplified method.

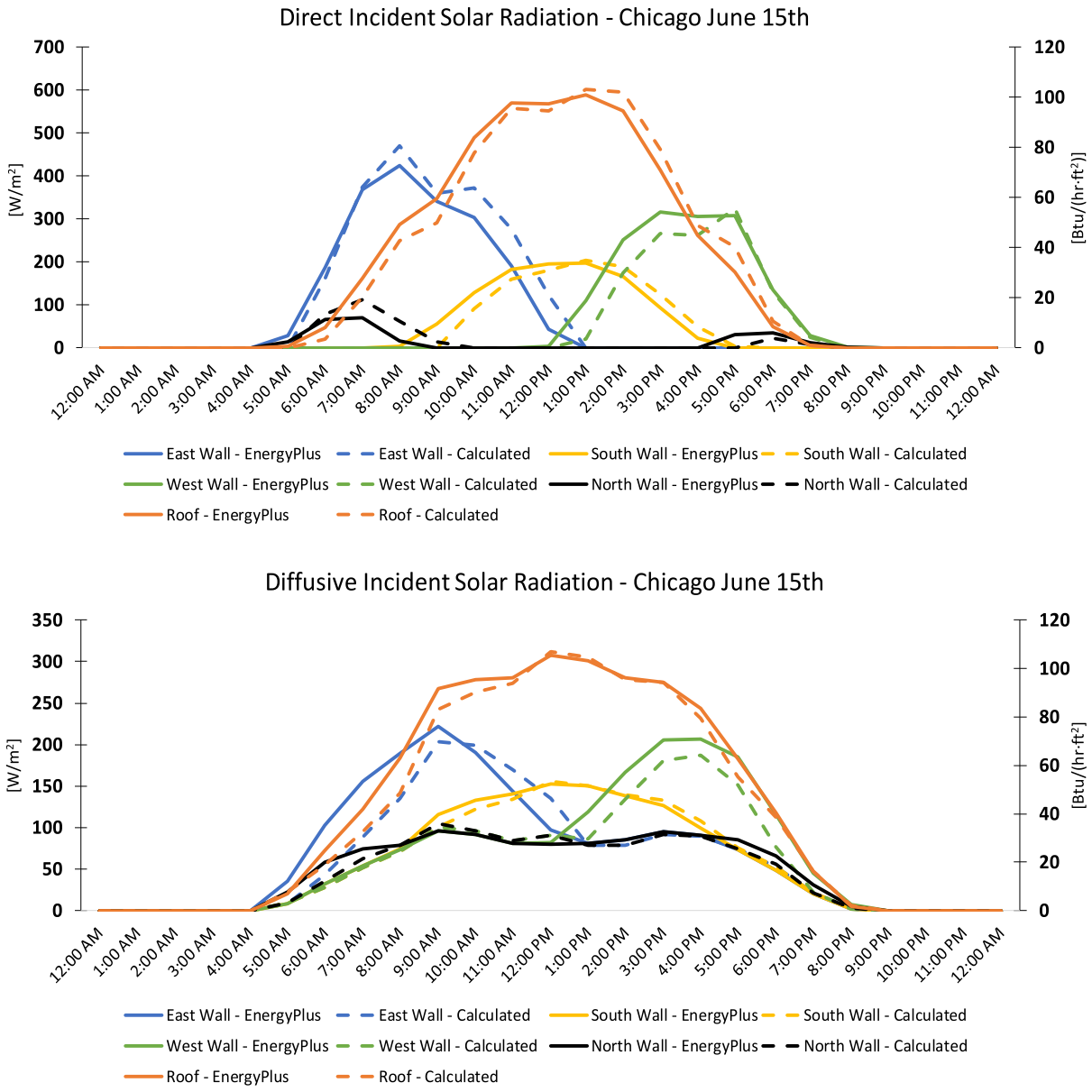

Fig. 2 Comparison of computed solar loads in EnergyPlus and the methods presented in this study. The comparison represents a summer day simulated for Chicago climate.

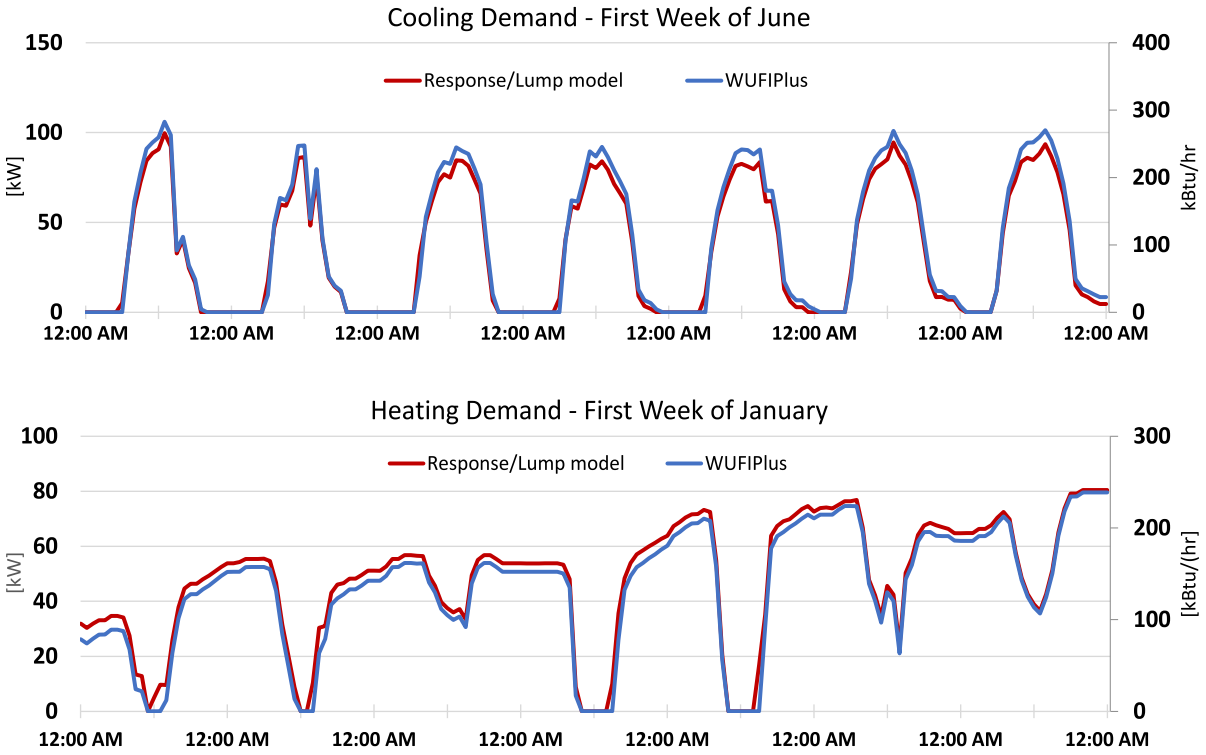

Fig. 3 Comparison of heating and cooling demand for a medium office building simulated in the climate of Atlanta, GA, USA. The comparison is made between the simulation result generated by WUFIPlus and the simplified response/lump model of this paper.

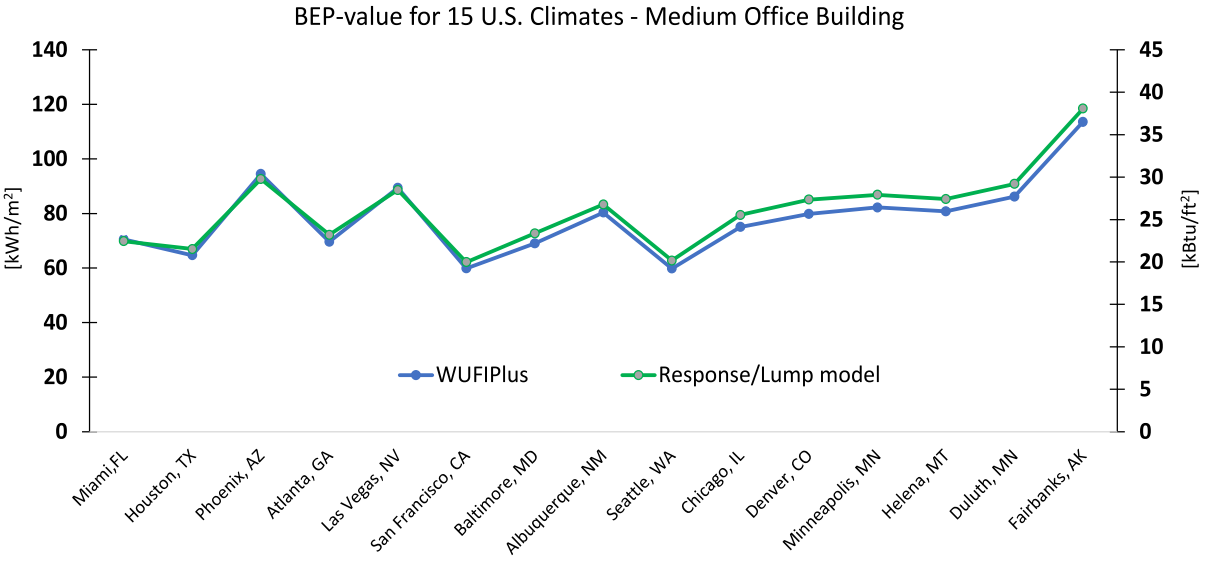

Fig. 4 Variation in BEP-value between 15 climates in the U.S. for a medium office building. The comparison is made between the simplified method and WUFIPlus simulations.

3. Results

3.1 Variations in BEP-Value between DOE Commercial Prototype Buildings and Various U.S. Climate Zones

The BEP-value is defined to represent the overall energy performance of the building envelope. Here, we use the 16 DOE prototype buildings [6, 30] to evaluate how BEP differs between various buildings, while constructed in the same climate. The thermal and geometric characteristics of the prototype buildings are given by the Building Energy Codes Program (EnergyCodes, 2020). The result of this effort is presented in Fig. 5.

In order to investigate the impact of air leakage on the BEP-value, two cases are depicted in Fig. 5: one with an assumed airtight building (Airtightness→∞), and one with an airtightness of 1.07 L/(s·m^2) at 75 Pa air pressure difference. Between the 16 prototype buildings, the assigned airtightness level increases the BEP-value with about 10% on average.

Further, three selected buildings are simulated in 15 different U.S. climate zones. The simulated buildings are medium office, high-rise apartment and warehouse. The variations in BEP-value for the three buildings and in the 15 climate zones are presented in Fig. 6.

As seen in Fig. 6, the BEP-value varies significantly depending on the type of building. All three buildings are simulated using the same energy code requirements [31], and with an airtightness of 1.07 L/(s·m^2) at 75 Pa air pressure difference. However, there are differences in geometry between the three buildings including the window-to-wall ratios. Despite these variations, there is a significant trend seen in for all three building types. The BEP-value is the highest in the coldest climate (8A) and the lowest in the temperate climate of San Francisco (3C).

3.2 Thermal Properties and Thermostat Setpoints

In this section, the BEP-value is used to study the impact of thermal mass and thermostat setpoints. In many situations, the thermostat setpoint temperature range is positively correlated with the impact from thermal mass on the energy demand [32]. Actually, the nonexistence of a difference in cooling and heating setpoints, eliminates the benefits of the thermal mass on energy demand. However, the thermostat setpoint temperature can significantly impact the energy demand, regardless of the presence of internal mass.

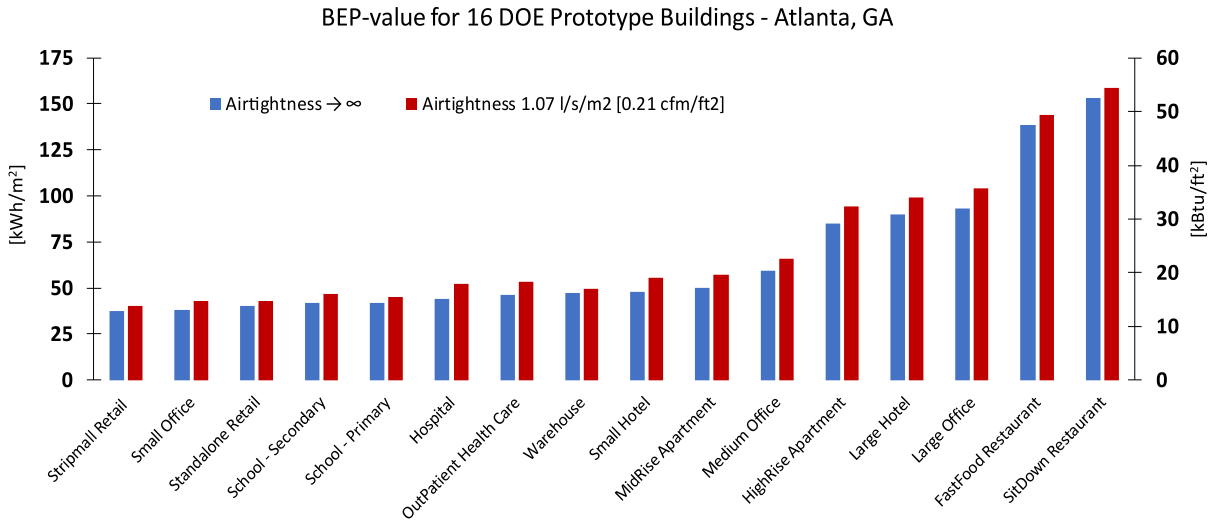

Fig. 5 Variations in BEP-value between 16 DOE prototype buildings [6, 30]. All buildings are simulated in the climate of Atlanta, GA.

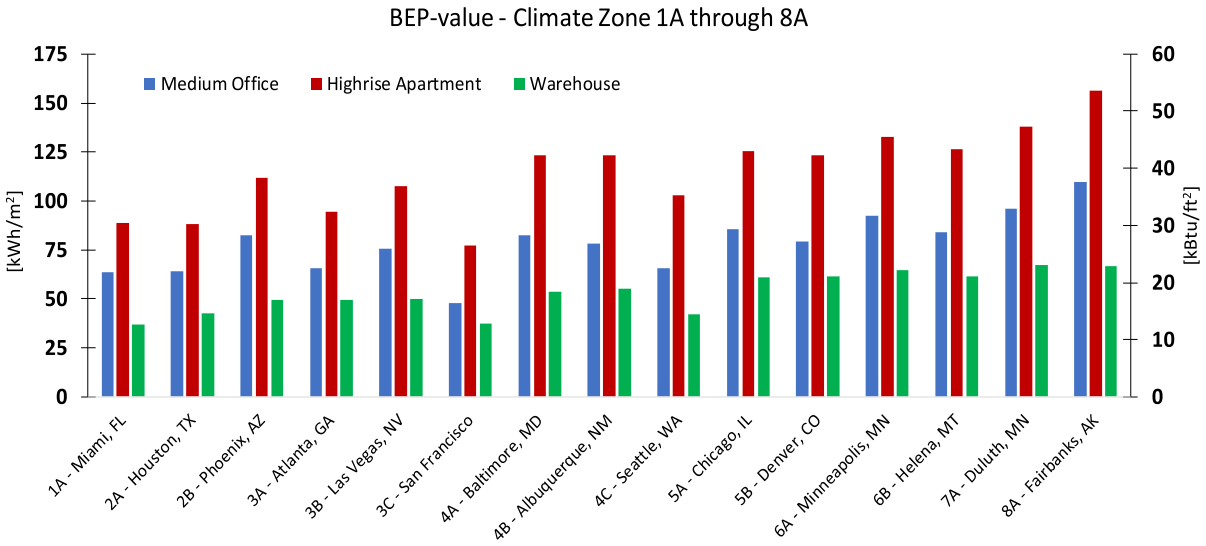

Fig. 6 Variations in BEP-value for three different types of buildings and 15 different U.S. climates.

Table 1 Specific heat levels for internal mass.

Case	Level	Heat capacity (kJ/K)
I	Very low internal mass	80 · Afloor
II	Low internal mass	110 · Afloor
III	Medium internal mass	165 · Afloor
IV	High internal mass	260 · Afloor
V	Very high internal mass	370 · Afloor

Table 2 Thermostat temperatures ranges between cooling and heating setpoints.

Case	Range	Setpoints (°C)
A	Small	22.8/21.1
B	Medium	23.3/20.6
C	Large	23.9/20.0

Typically, the more "widely" the indoor temperature is allowed to float, the less the energy demand. However, this theory very much depends on the outdoor temperature and thermal loads. Here, we will use the BEP-value to study in which U.S. climates thermal mass and setpoint temperature have the largest impact on the energy demand.

For this effort, we are analyzing the BEP-value for a Medium Office Building using 816 sets of TMY3 U.S. climate data [30]. The building insulation levels agree with that of International Energy Conservation Code (IECC) 2016 for climate zone 5A [33]. For each climate we are simulating 15 cases: five variations in level of internal mass, and three different ranges of indoor setpoint temperatures. The five levels of internal mass are applied according to Section 12.3.1.2 in ISO 13790 [34], as seen in Table 1. For thermostat temperatures, the ranges simulated are given in Table 2.

The 15 simulation cases are simulated in all 816 climate locations, resulting in 12,240 simulations.

First, we will investigate how the impact of internal mass varies in U.S. climates. While remaining the setpoint temperature range fixed to the lower range (case a), the variation in BEP-value is studied while alternating the level of internal mass. In Fig. 7, the relative importance over the U.S. is depicted. Here, a value of "1" indicates the highest relative importance between very low and very high internal mass for the specific location. A value of "0" means the lowest impact. Further, using the BEP-values from the simulation results, the absolute difference in energy demand between very low and very high internal mass is illustrated in Fig. 8.

Figs. 7 and 8 must be viewed somewhat differently. Since Fig. 7 illustrates the relative impact of internal mass on a scale from "0" to "1", a high value means that internal mass may reduce the energy demand significantly. According to the figure, areas along the

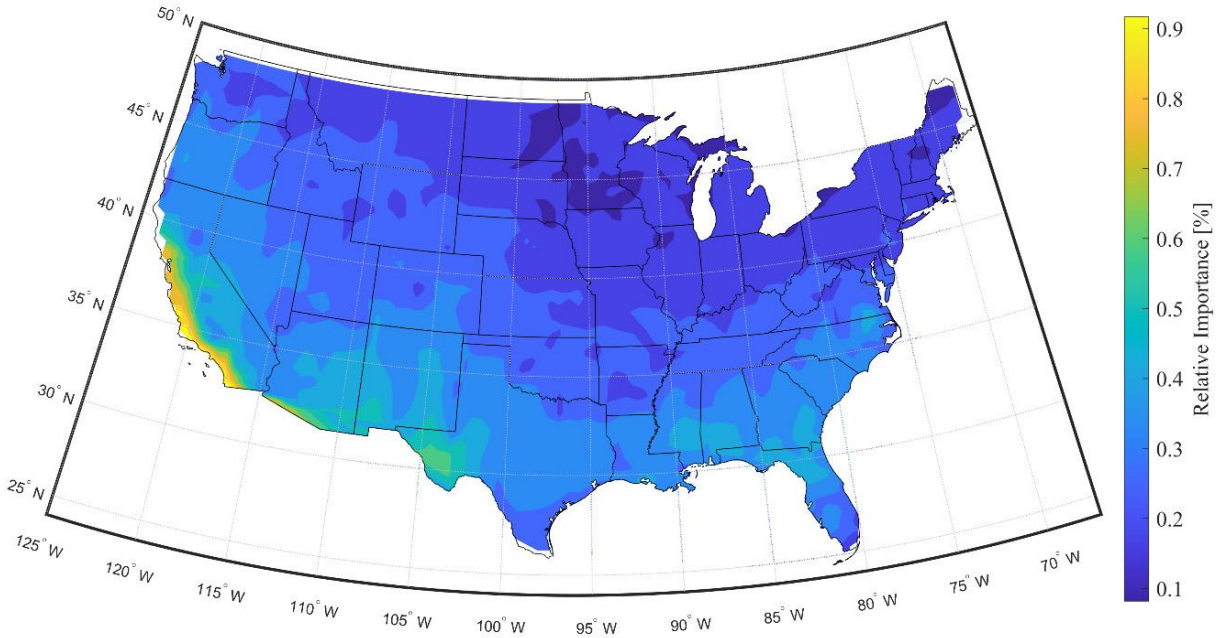

Fig. 7 Relative importance of internal mass. Locations with high importance have values closer to "1", while locations where internal mass is less important have values closer to "0".

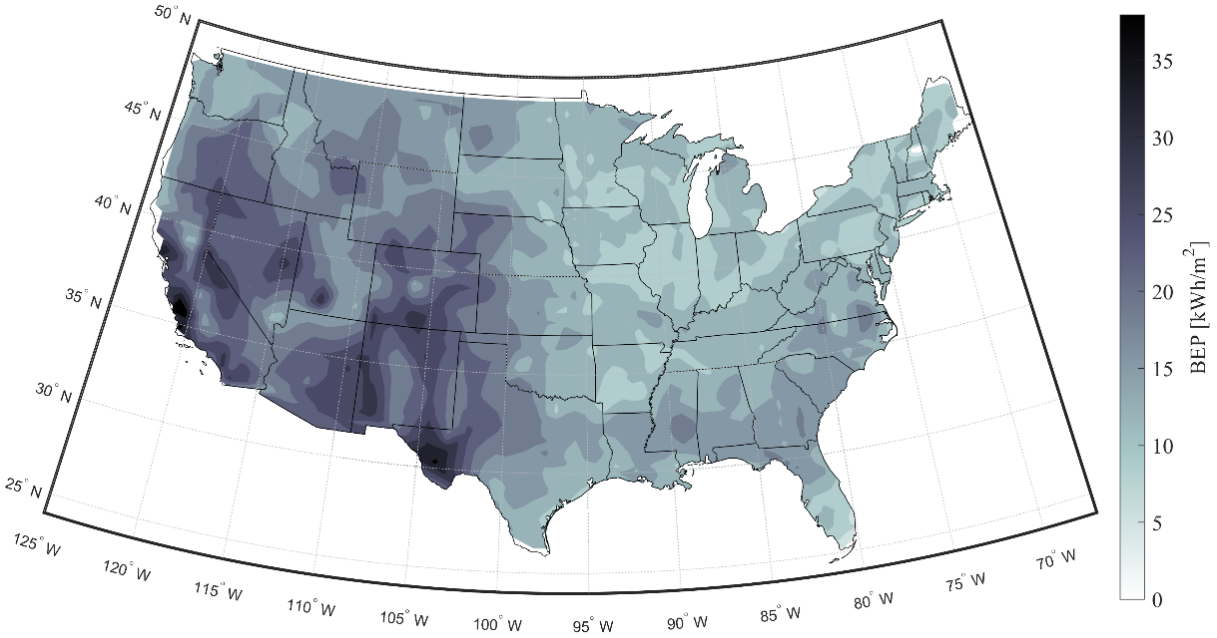

Fig. 8 Absolute importance of internal mass presented in reduction in BEP-value. Darker areas of the map indicate locations where internal mass holds a significant impact on the overall energy demand. Areas with brighter colors are locations where internal mass is less significant.

coast of California reveal most significance. However, exactly how much of a decrease a high internal mass contributes to at these locations are not reflected upon in Fig. 7, but instead Fig. 8. In this figure, locations with the most absolute decrease in BEP-value, thus energy demand, are given a darker color. In Fig. 8, we can see that internal mass notably impacts the energy demand in most Western regions of the United States.

According to the figure, internal mass can decrease the BEP-value by up to 37 kWh/m^2, year for the simulated medium-sized office building.

For the relevance of thermostat temperature ranges on the energy demand, the impact is not only dependent on the span between cooling and heating setpoints, but also the mid-point temperature between setpoints. For this study, the mid-point temperature for all cases is 21.9 °C. In theory, an exterior climate, including exterior and internal thermal loads, resulting in diurnal swings in temperatures around the mid-point, will generate optimized energy savings from allowing the indoor temperature to float [35]. Since a fixed mid-point is assumed for this study, assumingly certain climates will allow for larger impact than others. In order to somewhat reduce the impact of the selected mid-point temperature, the variation in BEP per temperature unit is instead studied by comparing the BEP-value between case (a) and (b) (22.8/21.1 °C and 23.3/20.6 °C). Fig. 9 represents the relative impact of the setpoint temperature range, and Fig. 10 depicts the impact of BEP-value per degree change in setpoint temperature.

As seen in Fig. 9, and similar to what is depicted in Fig. 7, the coastline of California is relatively most influenced by the range in thermostat temperatures. However, most Southern and coastal regions indicate a clear significance of thermostat setpoints. The actual impact on the energy demand per degree change in thermostat setpoint temperature is given in Fig. 10. Obviously, widening the setpoint temperature range will always result in a less energy demand due to increasing the span for which the indoor temperature can float. However, what Fig. 10 reveals, are those locations for which there are more annual cases of diurnal variations in indoor temperatures between the upper and lower setpoints. Thus, these locations benefit more from a wider range of thermostat setpoints.

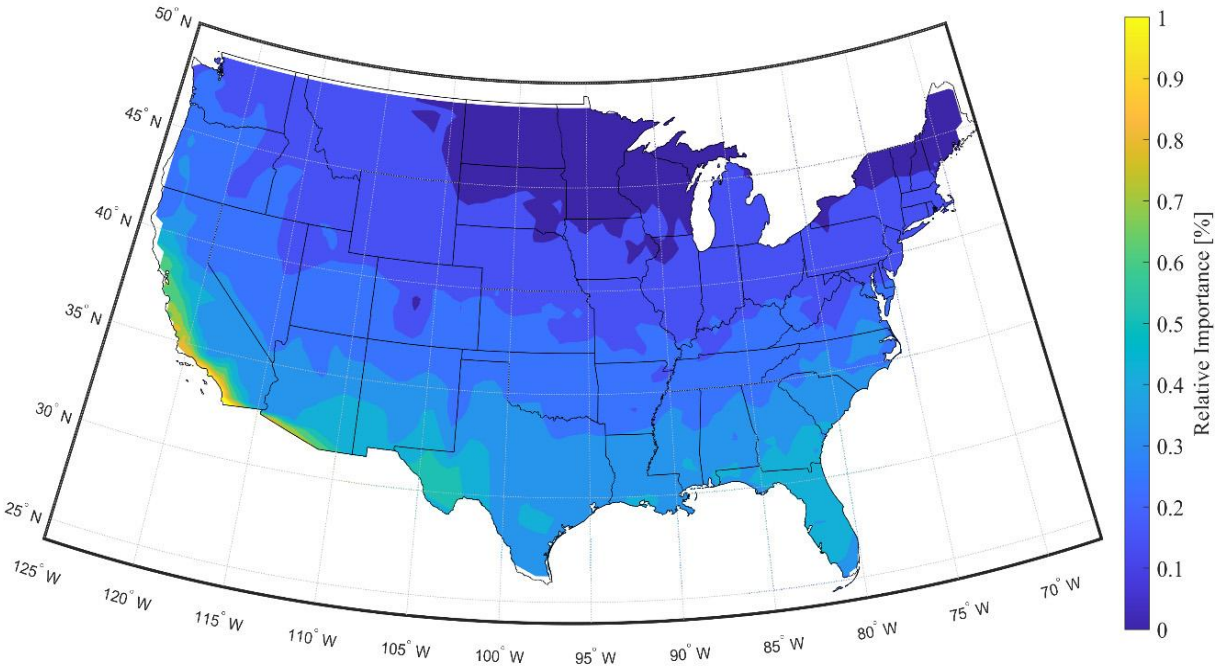

Fig. 9 Relative impact of the thermostat setpoints on the overall energy demand for a medium office building. The energy demands in areas with colors closer to green and yellow are more affected by changes in setpoint temperatures compared to area specific energy demands.

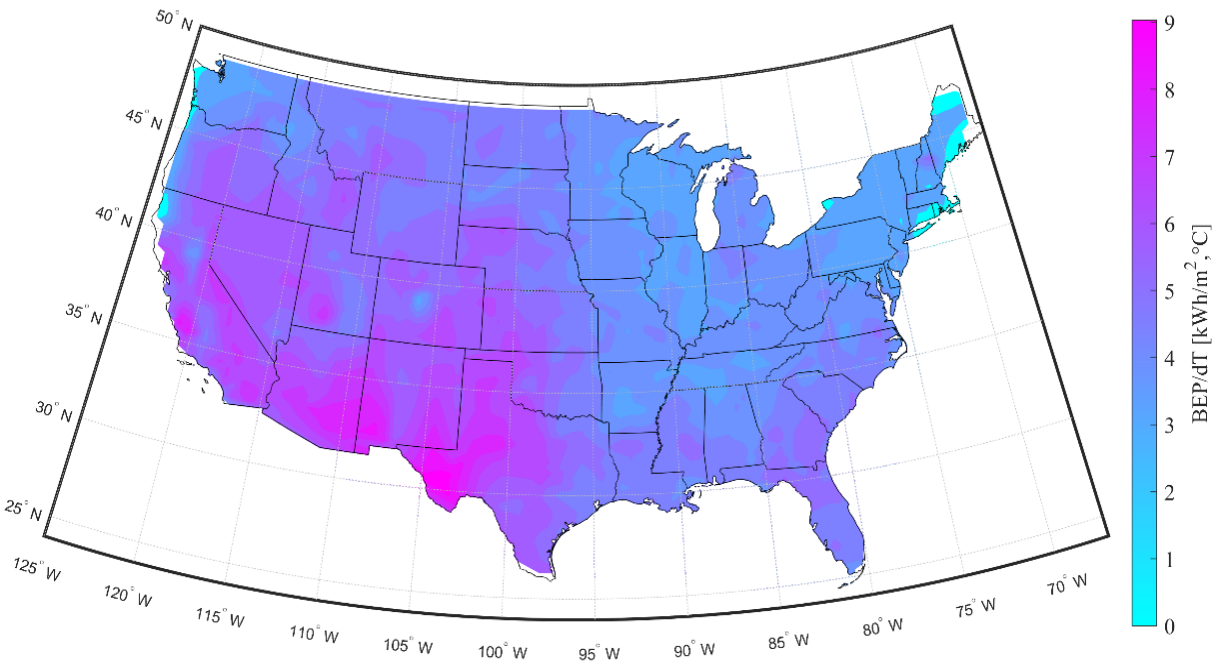

Fig. 10 Change in BEP-value per degree change in thermostat setpoint temperature.

4. Discussion

The BEP-value is proven to be representative to that of the overall thermal performance of the building envelope. By analyzing the BEP-value for various building types, Fig. 5 reveals that the metric will vary greatly, for a given climate, depending on the thermal properties of the building. Also, Fig. 6 depicts how much the thermal BEP varies for different U.S. climate zones.

This paper also shows how the impact of various building thermal properties is accounted for in the BEP-value. Figs. 7 and 8 illustrate the importance of internal mass on the overall energy demand across the U.S. These two figures reveal that many buildings located in the U.S.A. can significantly benefit from internal mass. The areas where internal mass matters the most on the overall energy demand are mainly located in the western part of the country. Still, thermal mass can be of importance for many other areas as well. Locations where internal mass matters the least are northern climates such as 6A and colder. Even, for very hot climates, such as 1A and hot 2A climates, internal mass matters less.

Further, this paper uses the BEP-value to evaluate the importance of thermostat setpoint temperatures and its ability to float on the overall energy demand. According to Figs. 9 and 10, these locations across the U.S. are about the same as for where internal mass is of the greatest benefit, in other words, most coastal, southern, and mid-west climates.

5. Conclusions

This paper defines and describes the computation of a new building envelope thermal performance metric, the BEP-value. Unlike other similar metrics, this metric accounts for the heat transfer mechanisms that are most relevant for the performance of the building envelope. These mechanisms include conductive heat transfer, air infiltration, and solar heat gains. The BEP-value is thus able to compare the envelopes of buildings with different use types in a fair manner. BEP procedures do not necessarily require the iterative simulation procedures that are typically part of whole-building calculations. Instead, the proposed metric relies on input data given by the geometry of

the building, thermal characteristics, and outdoor climate date. This feature allows for a quick, yet accurate, thermal performance assessment of a building envelope.

A simplified method for the calculation of the BEP-value is detailed. The method is a transient response and lumped analysis model. The metric may be calculated using more general building energy modeling software, but this is not required. A validation study of the metric is conducted by comparing simulation results from general-purpose whole building energy simulation tools with BEP calculations. This comparison demonstrates that the BEP-value gives overall predictions of energy performance comparable to results from existing simulation tools.

Finally, to demonstrate the use of the BEP-value to assess the thermal performance of the building envelope, several investigations into performance relative to U.S. climates are conducted. The influence of infiltration, internal thermal mass and thermostat setpoint is investigated and the impact of climate is explored using the BEP-value. The result of the analyses is presented using U.S. maps and allows the reader to identify in which areas of the country for which thermal mass and thermostat setpoints/setbacks matter most on the overall energy performance. In addition, these analyses demonstrate the ease of use of BEP as a means to compare the thermal performance of buildings with different building types, characteristics, and locations. Particularly, this ease of use is important in the exploration and assessment of potential retrofits.

Future work on the BEP metric is in progress. Using the BEP metric to design for building envelope characteristics and the impact of thermal comfort intervals and thermal mass on commercial buildings in U.S. climates have been studied [36].

Acknowledgments

This manuscript has been authored by UT-Battelle LLC under contract DE-AC05-00OR22725 with the US DOE (Department of Energy). The US government retains and the publisher, by accepting the article for publication, acknowledges that the US government retains a nonexclusive, paid-up, irrevocable, worldwide license to publish or reproduce the published form of this manuscript, or allow others to do so, for US government purposes. DOE will provide public access to these results of federally sponsored research in accordance with the DOE Public Access Plan (http://energy.gov/downloads/doe-public-access-plan).

References

[1] Christian, J. E., and Kosny, J. 1996. “Thermal Performance and Wall Ratings.” *ASHRAE* 38 (3).

[2] Ferrari, S., and Zanotto, V. 2016. “Approximating Dynamic Thermal Behaviour of the Building Envelope.” In *Building Energy Performance Assessment in Southern Europe*, edited by Ferrari, S., and Zanotto, V. Cham: Springer International Publishing, pp. 21-33.

[3] Godfrey, R. D., Wilkes, K. E., and Lavine, A. G. 1979. “A Technical Review of the ‘M’ Factor Concept.” In Proceedings of the Conference on the Thermal Performance of the Exterior Envelopes of Buildings, Kissimmee FL, 3-5 December 1979, pp. 472-89.

[4] Kosny, J., Kossecka, E., and Desjarlais, A. O. 1998. *Dynamic Thermal Performance of Concrete and Masonry Walls*. pp. 629-43.

[5] Moody, S. S., and Sailor, D. J. 2013. “Development and Application of a Building Energy Performance Metric for Green Roof Systems.” *Energy and Buildings* 60: 262-9.

[6] EnergyPlus. “EneryPlus Engineering Reference.” https://energyplus.net.

[7] Logue, J. M., Turner, W. J., Walker, I. S., and Singer, B. C. 2016. “A Simplified Model for Estimating Population-Scale Energy Impacts of Building Envelope Air Tightening and Mechanical Ventilation Retrofits.” *Journal of Building Performance Simulation* 9 (1): 1-16.

[8] Alterman, D., Moffiet, T., Hands, S., Page, A., and Luo, B. 2012. “A Concept for a Potential Metric to Characterise the Dynamic Thermla Performance of Walls.” *Energy and Buildings* 54: 52-60.

[9] Arkar, C., and Perino, M. 2019. “Dynamic Thermal Performance Metrics for Adaptive Building Constructions.” In *Proceedings of Building Simulation 2019*, January 2019, pp. 330-5. doi: 10.26868/25222708.2019.210474.

[10] Reilly, A., and Kinnane, O. 2017. "The Impact of Thermal Mass on Building Energy Consumption." *Applied Energy* 198: 108-21.

[11] American Society of Heating Refrigerating and Air-Conditioning Engineers. 1975. *Standard 90-1975, Energy Conservation in New Building Design*. Atlanta.

[12] Yik, F. W. H., and Wan, K. S. Y. 2005. "An Evaluation of the Appropriateness of Using Overall Thermal Transfer Value (OTTV) to Regulate Envelope Energy Performance of Air-Conditioned Buildings." *Energy* 30: 41-71.

[13] Vijayalaxmi, J. 2010. "Concept of Overall Thermal Transfer Value (OTTV) in Design of Building Envelope to Achieve Energy Efficiency." *International Journal of Thermal & Environmental Engineering* 1 (2): 75-80.

[14] Wilcox, B. 1991. "Development of the Envelope Load Equation for ASHRAE Standard 90.1." *ASHRAE Transactions* 91 (2): 913-27.

[15] 1989. *Energy Efficient Design of New Buildings except Low-Rise Residential Buildings*. Technical Report. Atlanta, GA: American Society of Heating, Refrigerating and Air-Conditioning Engineers, Inc.

[16] O'Callaghan, P. W., and Probert, S. D. 1977. "Sol-Air Temperature." *Applied Energy* 3 (4): 307-11.

[17] Spitler, J. D., McQuiston, F. C., and Lindsey, K. L. 1993. "The CLTD/SCL/CLF Cooling Load Calculation Method." *ASHRAE Transactions* 99 (1): 183-92.

[18] Spitler, J. D., Fisher, D. E., and Pedersen, C. O. 1997. "The Radiant Time Series Cooling Load Calculation Procedure." *ASHRAE Transactions* 103 (2): 503-15.

[19] Wang, N., Goel, S., Makhmalbaf, A., and Long, N. 2018. "Development of Building Energy Asset Rating Using Stock Modelling in the USA." *Journal of Building Performance Simulation* 11 (1): 4-18.

[20] Shamsi, M. H., O'Grady, W., Ali, U., and O'Donnell, J. 2017. "A Generalization Approach for Reduced Order Modelling of Commercial Buildings." *Energy Procedia* 122: 901-6.

[21] ISO. 2017. "Thermal Performance of Buildings—Transmission and Ventilation Heat Transfer Coefficients—Calculation Method." *ISO 13789:2017*, ISO (International Organization for Standardization) Copyright Office.

[22] Hagentoft, C.-E., and Pallin, S. 2020. "Thermal Step Response of N-Layer Composite Walls—Accurate Approximative Formulas." *Journal of Heat Transfer* 142 (3): 034502. https://doi.org/10.1115/1.4045642.

[23] Shampine, L. F., and Reichelt, M. W. 1997. "The Matlab Ode Suite." *SIAM journal on Scientific Computing* 18 (1): 1-22.

[24] Kreyszig, E. 2007. *Advanced Engineering Mathematics*. New York: John Wiley & Sons.

[25] ASHRAE. 2017. "ASHRAE Handbook—Fundamentals—Chapter 16 Ventilation and Infiltration." *16.10*. Dayton, OH: American Society of Heating, Refrigerating and Air-conditioning Engineers, Inc.

[26] Fraunhofer-IBP. "EneryPlus Engineering Reference." https://wufi.de/en/software/wufi-plus/.

[27] Perez, R., Ineichen, P., Seals, R., Michalsky, J., and Stewart, R. 1990. "Modeling Daylight Availability and Irradiance Components from Direct and Global Irradiance." *Solar Energy* 44 (5): 271-89.

[28] EnergyCodes. "Commercial Prototype Building Models." https://www.energycodes.gov/development/commercial/prototype_models.

[29] ASHRAE. 2019. "ANSI/ASHRAE/IES Standard 90.1-2019—Energy Standard for Buildings except Low-Rise Residential Buildings."

[30] EnergyPlus. "Weather Data by Region—All Regions—North and Central America WMO Region 4—USA." https://energyplus.net/weather-region/north_and_central_america_wmo_region_4/USA.

[31] IECC. *International Energy Conservation Code—Residential Energy Efficiency*. Washington DC: International Code Council, Inc.

[32] Verbeke, S., and Audenaert, A. 2018. "Thermal Inertia in Buildings: A Review of Impacts across Climate and Building Use." *Renewable and Sustainable Energy Reviews* 82: 2300-18.

[33] IECC. 2015. *International Energy Conservation Code—Residential Energy Efficiency*. Washington DC: International Code Council, Inc.

[34] ISO. 2007. "Energy Performance of Buildings—Calculation of Energy Use for Space Heating and Cooling." *ISO/FDIS 13790:2007*, ISO Copyright Office.

[35] Hagentoft, C.-E., and Pallin, S. 2020. "A Conceptual Model for How to Design for Building Envelope Characteristics. Impact of Thermal Comfort Intervals and Thermal Mass on Commercial Buildings in U.S. Climates." *Journal of Building Engineering* 35 (3): 101994.

Journal of Civil Engineering and Architecture 15 (2021) 318-329
doi: 10.17265/1934-7359/2021.06.004

Modular Disruption in Construction Industry—The Environmental Benefits

Dimitra Tzourmakliotou

Department of Civil Engineering, Democritus University of Thrace, Xanthi 67100, Greece

Abstract: The impact of Covid-19 on every aspect of life is undeniable. As the pandemic began to spread throughout February 2020, no one could have foretold the ways in which this disease would change society. One of the key things that the Covid-19 pandemic has accelerated is off-site manufacturing and the different ways in which modular construction can be utilized to deal more effectively with the demands of a crisis. The rapid erection of modular hospitals across the globe has been critical in fighting the outbreak of Covid-19, not least the modular hospital in Wuhan that was built in just 10 days. Modular construction was already a hot topic for the industry, the pandemic has simply enhanced this—and the last few months were given the opportunity to explore the options in more detail. There is no doubt that modular construction will continue to play a part in construction projects in the longer term and construction industry should adapt to accommodate this change. Since construction industry is the largest consumer of natural resources, this article would emphasize on the sustainability dimensions of modular construction and its performance during the whole lifecycle. A thorough literature review of the sustainability benefits of modular construction compared to its tradition counterpart is presented.

Key words: Off-site construction, modular construction, environmental benefits, sustainability.

1. Introduction

Modular construction may seem like a new building method, yet it is actually been used for a long time. Its roots can be traced to the Rome in AD-43, where the Romans used modular building elements to build their forts quickly and efficiently as they realized that these forts and stockades used a large number of same and repeating components. However, not only the Romans, but the Britishers also transported simple modular houses by ships to their new settlements in the colonies to provide comfortable European Style living to its officers in these colonies. In 1840s modular construction made its way to the United States in response to the housing needs of the California Gold Rush, prefabricated houses were transported from New York to California [1].

One of the most famous examples of early modular construction is Crystal Palace, built for Britain's Great Exhibition of 1851. Designed in less than two weeks, it utilized light and inexpensive materials such as iron, wood and glass, and was constructed in only a few months [2]. Afterward, Crystal Palace was dismantled, moved, and rebuilt at another location [3]. Another example of modular construction is the Eiffel Tower. Eiffel Tower was built as a temporary exhibit structure for the Centennial Exhibition in Paris in the year 1889 for the celebration of the French Revolution of 1789. The Eiffel Tower consists of modular iron parts that were mass produced at an off-site location on the outskirts of Paris [4]. Each of the 18,000 iron parts used to construct the Tower was specifically designed and calculated, traced out to an accuracy of a tenth of millimeter and then put together forming new pieces around 5 m each. These pieces were then taken to the site and assembled to build a 300-m tall structure which completed in a time period of just over two years.

Corresponding author: Dimitra Tzourmakliotou, Ph.D. in civil engineering, associate professor in Democritus University of Thrace, steel structures, space structures, design for deconstruction, sustainability of steel structures.

However, the first true catalyst for modern modular construction happened shortly after the turn of the 20th century. Starting in 1908, Sears, Roebuck, and Co. sold modular houses through its Sears Modern Home Program. The concept was simple: Order one of the 400 house plans from the catalog and receive it in easy-to-construct sections [5, 6]. In the mid-1940s, the industry turned to modular when faced with skyrocketing demand for new homes after World War II and, in the late 1950s, modular expanded into the construction of schools and medical facilities [7, 8]. In the 1960s and 1970s high rise concrete modular construction was introduced. The Hilton Palacio del Rio Hotel was among the first concrete high rise modular buildings in the world. The 500-room hotel was designed, completed and occupied in an unprecedented period of 202 working days. The hotel's room modules were pre-cast from light-weight structural concrete [9]. Nowadays, based on the spread of modular construction we can categorize countries into three groups: those that have an acknowledged high application of prefabricated housing such as Sweden (84% of all detached homes) and Japan (28%); those that have been identified as having both relatively high levels of prefabrication and highly efficient traditional or "craft based" house-building industries such as Germany (9%) and the Netherlands (20%) and major economies that have an infrequent application of prefabricated housing such as the United States (5%), United Kingdom, and Australia [10].

2. Sustainability in Construction Industry

The construction industry strongly affects the economy, the environment and society as a whole. It touches the daily lives of everyone, as quality of life is heavily influenced by the built environment surrounding people. The construction industry accounts for 13% of global GDP (Gross Domestic Product) and is using the natural resources 1.5 times faster than the world can replenish itself. The construction industry is the world's largest consumer of energy, resources and raw materials as it consumes about 50% of the total global raw resources for the manufacturing of building products worldwide [11, 13, 15]. Also, it accounts for more than 40% of the world's energy use and is attributable for 30% of global greenhouse gas emissions [11, 12, 14]. In Europe, the construction sector uses by far the greatest amount of resources in the economy on a mass basis, and consumes between 5% and 10% of total energy only for the production of construction materials [16-19]. Moreover, a large volume of CDW (construction and demolition waste) is generated by the construction industry each year, which in industrialised countries can be up to 60% of the total amount of solid waste generated by mass [20-24]. In Europe, CDW accounts for 38% of Europe's total solid waste generated, excluding wastes from the mining and quarrying activities [18, 21, 25, 26]. Also, the construction industry in EU generates 40% of the carbon dioxide CO_2 emissions and uses 50% of all-natural resources. Furthermore, global demographic and lifestyle changes, growth in the world's population and, in particular, its middle classes, which will expand from two to five billion by 2030, are increasing the existing demand in construction industry while it is under increasing pressure to minimize its environmental impact.

Sustainability could help the construction industry to reduce its environmental footprint, and to avoid rising costs, labour shortages, delays, and other consequences of volatile commodity markets but that is something that has been put somewhat on the backburner for the time being due to disruption caused by the Covid-19 crisis. As an industry, so often the focus is on cost and designing to meet the minimum standards rather than considering the longer-term impact of the construction on the environment. Modular construction would involve reshaping the way projects are procured, designed, constructed, operated and repurposed.

3. Modular Construction

Since its introduction stateside, the process of constructing structures off-site, then transporting and assembling them in half the time compared to traditional techniques, has undergone significant technological innovations, including advances in associated software, automation and building information modeling. This blend of technological prowess plus modularity is a key feature for enhancing sustainability in construction.

Modular construction is more of a manufacturing process than it is a typical construction. The modules (frames, walls, ceilings, floors, etc.) are all produced in a factory, or what we would call "off-site". Compared to a traditional construction site, where hundreds of processes are happening at the same time, this highly centralized process allows for closer inspection and quality assurance. Flaws in material quality are flagged directly at the source of manufacturing and resolved before ever reaching the site, ensuring the minimization of waste on site, the strictest compliance to building codes and higher safety standards once the construction phase has begun. Moreover, because modular components are so highly standardized and predictable, it is possible to model and pre-optimize facilities in the virtual 3D space with total detail and accuracy, simulating everything from airflow and human movement to asset performance and energy consumption.

The terms off-site construction, prefabrication, and modular construction are used interchangeably and cover a range of different approaches and modular systems. These modular systems vary depending on the complexity of the elements being brought together as explained below.

4. Categories of Modular Systems

Panelized Systems ("2-Dimensional"): also regarded as "non-volumetric preassembly" these are either classified as "open" or "closed". The open panels normally delivered to site purely as a structural element with services, insulation, cladding and internal finishes installed in situ while the closed panels apart from the structural elements usually include more factory-based fabrication such us lining materials and insulation and may even include external cladding, internal finishes, services, doors, and windows [27, 28]. Using this panelized system's parts of the walls, ceiling or roof can be constructed in a factory and rapidly assembled on site by an experienced construction team to form the completed building. These are components that can be flat packed, that is grown up into a full-sized building.

Modular or Volumetric System ("3-Dimensional"): involves three-dimensional modules that can be in isolation or in multiples to form the structure of the building. These systems are pre-engineered and pre-assembled units in the factory which can be transported to site and fitted into an existing building or incorporated into a traditional construction project with limited amount of work on site [29-32]. A 3D volumetric approach delivers the potential for maximum efficiencies and time savings—but the trade-offs include transportation costs and size limitations. The time savings onsite need to be substantial for volumetric systems to be chosen over panelized. The most common volumetric system is a bathroom pod. The bathroom pod contains all the sanitary ware, electrical and plumbing fittings and even the finished tiles. This entire unit can then be transported to the construction site, installed and can be made instantly ready for use. Additionally, this can include "complete buildings" where the completed useable space forms part of the completed building or structure finished internally (lined) and externally (clad). A 3D volumetric approach is most suitable for projects with a high level of repeatability and a high ratio of wet to dry rooms.

Hybrid System (2D + 3D). A hybrid system is a combination of more than one discrete system or approach and is normally a combination of both volumetric and panelized systems. This approach

combines the flexibility and logistic advantages of 2D panels with the productivity benefits of 3D modules [29, 31, 33, 34]. Typically, wet areas are manufactured as bathroom pods, while the remainder of the building is made from 2D panels. However, the manufacturing process required to deliver both solutions becomes more complex, as does coordination of the supply chain.

Sub-assemblies (Component Systems 2D or 3D). Any major part of a building made in a factory and brought to the construction site can be classed as a sub-assembly, which forms part of a component system [29, 34-36]. These do not form the primary structure of the building. Foundation systems and cassette panels are typical examples. Sub-assemblies can be as small as locks and handles for the doors, or they can be larger components such as pre-assembled roof trusses. Sub-assemblies are likely to be used in a construction project that predominantly uses onsite techniques but enables some of the trickier components to be built in a factory that allows for more precision than the building site.

5. Benefits of Modular Construction

5.1 Schedule

The most important benefit of modular construction is the ability to substantially reduce the time needed for construction (Fig. 1). This diagram shows a side-by-side comparison of a timeline for a site-built construction vs. a timeline for a modular construction. The first two stages of construction are the same. The first major difference in timeline comes when the actual construction begins. With site-built construction, all site preparation and foundation work must be completed before the actual house can be built since the framing for the house must be built on top of a finished foundation. Using modular construction on the other hand, work on the factory can take place at the same time as the foundation is being prepared [37, 38].

Numerous projects have demonstrated that schedule savings are the most easily documented and noticeable savings that occurs because of modular construction. Parallel scheduling for off-site and onsite construction schedules saves 30% to 50% of project duration compared to stick-built traditional construction processes [39-41]. This is due to concurrent site and factory work, as well as factory production being faster than on-site framing, removing weather delays and subcontractor sequence delays associated with on-site construction [42-44]. This makes modular construction suitable for owners who need buildings quickly, properties with hard dates for occupancy such as the educational and health sectors, and areas where seasonal weather restricts or even halts construction [35, 45, 46]. Additionally, this time saving can reduce significantly the final cost

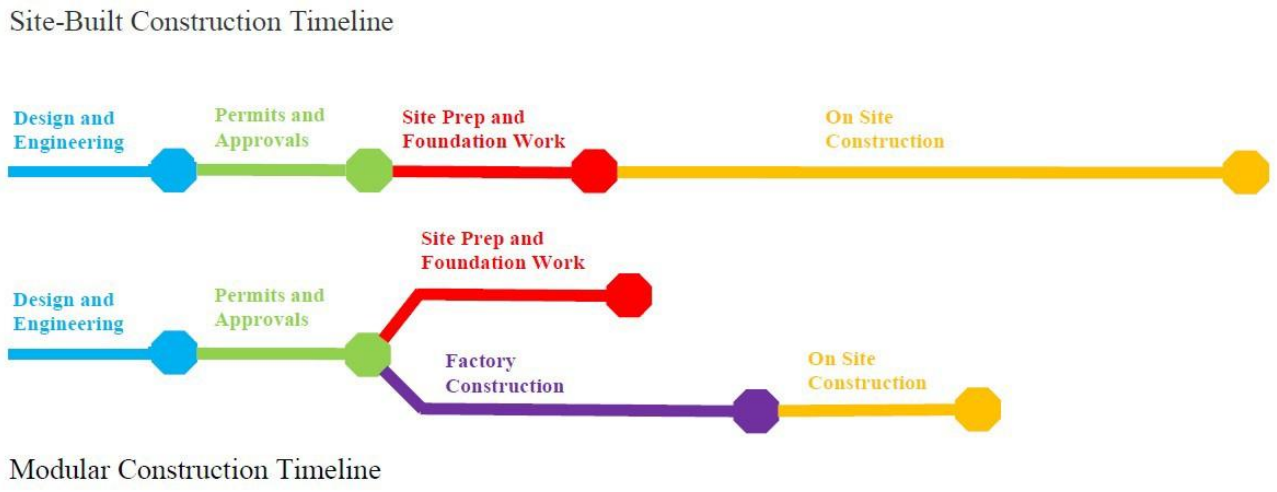

Fig. 1 Timeline of site-built construction vs. modular construction.

Table 1 Potential modular construction savings/cost (%).

	Pre-construction phase	Estimated savings/Cost (%)
Design	Preferably, a modular-based design philosophy should be adopted from the start, ensuring that various considerations—including those related to geometry and material strategies, transportation logistics, and issues related to shared scope and coordination—are fully integrated into the process. However, there is often an additional fee in the design due to a lack of experience in designing modular projects. But as the industry gains more experience in such projects and adjusts to producing repeatable designs that can be used and adapted multiple times, this cost will likely drop. The development of digital tools such as BIM (building information modeling) will also help in this direction [58]. In modular construction design includes structural design, detailing, 3D modelling, service layouts, soap drawing and is usually carried out by the modular supplier. So, the cost of design finally might be reduced by 3%-4% compared to traditional design cost [55, 65, 74, 75].	-3% to -4%
Site Overheads	Modular construction has already a proven track record of decreasing project timelines and construction risk which in turn minimizes the cost of site overheads and financial carrying costs (such as insurance, weather related issues). In traditional construction site preliminaries may account for 12% to 15% of overall cost while in modular construction it may be taken 7% to 8% [65, 75].	-5% to -8%
	Construction Phase	-8% to -10%
Materials	There are numerous factors which either increase or decrease the cost of materials for off-site manufacturing compared with onsite. Cost increase factors •As manufacturing facilities become more automated greater precision in the tolerances of the quality requirement for the materials needed which in turn can increase costs. •Due to transportation from the manufacturing facilities on-site some duplication of key structural elements such as beams and columns, is required in order to be structurally sound in situ whilst being raised and lowered throughout the handling process (transportation and assembly). This can substantially drive-up material costs depending on the material choice and level of design optimization. • The need for "standardization" means that some economy in use of materials is sacrificed for production efficiency. Cost decrease factors • Optimizing procurement for a factory rather than for individual projects the contractor can save the cost of material. Utilizing different methods, the cost can be decreased by about 20%. • By direct procurement and cut out of intermediaries. • Efficient ordering and optimized deliveries to reduce logistic cost. • Economies of scale for the purchasing of all units going through a factory versus individual projects. • Manufacturing process has far lower wastage rates than a construction site. Because of this it is difficult to be clear on whether material costs will be higher.	-3% to -4%
Labor Force (On- and Off-Site	The construction industry is experiencing a clear shortage in skilled and semi-skilled labor. Fewer younger workers are coming into the construction trades to replace those who are aging out. One of the most disruptive aspects of modular construction is the reduced labor force required during the construction phase as in a modular building, up to 80% of the traditional labor activity can be moved off-site to the manufacturing facility. Modular, construction lays the framework to optimize a shrinking labor force and maximize productivity. A modular construction company usually employs a group of full-time employees in the manufacturing facility to address all required off-site construction and manufacturing of the modules; a consistent workforce tends to make modular construction faster and of higher quality than traditional construction methods. In addition, as a modular construction approach requires more standardized, automated, and controlled operating environment of a factory and a high level of coordination and collaboration among project team members, it promotes a more integrated process that can in turn lead to increased productivity [75]. Conversely, onsite assembly of modules requires a lower-skilled and thus lower-cost labor force. Overall, it is expected transition to modular manufacturing to lower the labor cost on a project by up to 15%. Saving can be even more significant up to 10%, when high-value activities such as mechanical, electrical and plumbing (MEP) installation done off-site. Nowadays, modular manufacturers are growing, and 25% of firms in the 2018 Associated General Contractors (AGC) Workforce Survey [66, 67] reported adopting or increasing the use of methods like off-site fabrication to deal with labor shortages.	-15% to -25%

Table 1 to be continued

Logistics	Modular construction possesses the characteristic of both construction and manufacturing and a new tailored logistic process is necessitated for its future coherent operation. The modular components leaving the factory can be either 2D panelized systems or 3D volumetric or modular systems. In the case of 3D volumetric systems, the components are typically large and cumbersome requiring specific transportation considerations that might cause delays, incur extra cost and add complexity to the construction process [60, 62, 63, 64]. Therefore, a well-coordinated transportation plan, via specific routes at specific times, with adequate and specialized vehicles should be carried out in advance [60, 61]. Additional caution should be taken when they are carried out across public roads and urban areas [60]. Consequently, the contractors should take special care that the productivity gains offset this cost, carefully weighing wage differentials between the manufacturing facility and the product's end destination, as well as the distance involved in delivery. The total cost of a modular project can increase by up to 10% in locations with restrictive transport regulations [63, 65].	+10%
Rework	Quality assurance is one of the most vital aspects in almost every industry, and, when it comes to construction, it is "the" most vital aspect. Higher quality can be attained with the use of modular construction due to better manufacturing facilities in which the components are built, than on a construction site which has a big impact on rework. Rework refers to re-doing a process or activity that was incorrectly implemented. Rework is usually pure waste and substantially affects the schedule, cost, and quality of construction projects [68, 69]. A significant proportion of rework is caused by errors made during the design process [70]. The direct costs of rework on site are projected to be 2%-12% of the overall construction cost; therefore, rework should be managed effectively [71-73]. Modular construction due to stringent quality checks at every stage and much more restrictions in the design and construction can reduce or eliminate rework significantly improving construction schedules, potentially by up to several months and ensuring project cost. Moreover, as the modules should have enough strength and load bearing standards when transported by trucks, high quality materials which are durable, lightweight, and resistant to weather are required. This elevated material quality and manufacturing process is reflected in cost savings of 1% to 2% [75].	-1% to -2%
Financing	Modular construction is a relatively new concept and thus, the financing industry is just beginning to explore the opportunity and make themselves aware of this new system. But as they are in the early stages of their learning curve proposed lending schemes for projects utilizing modular construction tend to be higher since it is different from the stick-built construction and not always fully understood by the financing industry. However, this will change over time as a substantial track record and scale are established and greater research and development (R&D) is undertaken. As it is mentioned previously the most important benefit of modular construction is speed of construction and since time equals money, the ability to accelerate projects can lower costs. Even though upfront payment can be higher in modular construction, financing would be required for short time which in turn would reduce the project's financial cost by 2% to 5% [76, 77].	-2% to -5%
Factory Costs	The initial capital investment for the construction of the manufacturing facility and the running expenses of the production facility should be considered against the above-mentioned savings. Depending on the production facility the factory cost to be allocated can be between 5% and 10% of overall cost on a modular construction project [65].	+5% to +10%

of the project [47]. However, it should be mentioned that, when the number of stories in modular construction increases, the time savings decrease considerably as the project becomes more complex and subsequently additional engineering and communication as well as more work in the jobsite is required [48]. Nevertheless, the completion time of modular construction is still less than that of conventional ones even though the project is a high-rise modular construction [38].

5.2 Construction Cost

Although the costs of modular construction are often more predictable than with traditional construction methods this does not mean it will automatically result in savings in overall project cost. There are a series of factors that could result in modular construction savings as are referred in Table 1 [38, 49, 50]. Saving in modular construction costs can come either from the pre-construction (design and site preliminaries) or the construction phase (sub-structure, materials, on- and off-site labor, logistics) [42, 51-53]. Moreover, the manufacturing process involved in off-site construction eliminates the demand for subcontractors and the margins that they incorporate in their quotations. Nonetheless, the main trade-offs are among the savings in onsite labor compared to possibly higher costs for materials

and the increase in logistics costs. Modular construction also tends to have higher upfront design costs against lower costs for rework and redesign [54]. However, apart from the construction costs, there are two more aspects regarding the cost that are significant to consider: the full life-cycle costs and the impact that modular construction can have on them and the cost of the factory investment itself and how this influences the overall savings of modular construction.

6. Sustainability Benefits of Modular Construction

The implementation of modular construction in the built environment can have a substantial impact on efforts to achieve the "three pillars of sustainability, the so-called TBL (triple bottom line) that make up the three pillars of the framework, environmental, economic and social. These sustainability benefits of modular construction have been reported in many studies and are presented in Table 2. The benefits arise from the more efficient manufacturing and construction process [56, 57, 59], the improved in-service performance of the completed building, and the potential reuse at the end of the building's primary life due to the flexibility and durability of modular construction.

Table 2 Sustainability benefits of modular construction.

	Description	References
Economic Benefits	Speed of construction. Several activities can be performed simultaneously;	[37, 74, 75, 78, 79, 85, 86, 87]
	Economy of scale in manufacture, especially in larger projects (dependent on the production volume) or in repeated projects using the same modular specification;	[74, 75, 82, 83, 84]
	Saving in design costs due to the client as most of the detailed design is carried out by the modular supplier;	[74, 75]
	Reduced overheads in-site infrastructure and management of the construction process (known as site preliminaries) due to speed of construction;	[73, 75, 78, 79, 81]
	Compressed project schedules, leading to reduced site management costs for the main contractor and early return on investment for the client;	[32, 75, 78, 79, 81, 84, 85]
	High levels of consistency and higher product quality achieved by the factory based construction process and predelivery checks, leading to reduced rework or "snagging" costs;	[32, 58, 74, 75, 78, 97]
	Costly delays due to severe weather conditions can be eliminated;	[79, 88]
	Higher productivity in manufacture and less work on site, leading to reduction in labor costs and transportation per unit completed floor area;	[32, 58, 74, 75, 78, 89, 90, 97]
	Savings in material use due to rationalization of material orders;	[74, 78]
	Savings in disposal costs due to the reduced amount of waste;	[74, 78, 92]
	Receiving volume discounts by ordering materials in bulk;	[79]
Environmental Benefits	Reduced site and neighborhood disturbance during construction, which is important in urban areas where the adjacent buildings have to function without disruption;	[75, 78, 79]
	Reduced air & water pollution, dust & noise;	[78, 94]
	Better energy performance and decrease in CO_2 emissions due to reduced transportation of labor, materials and machinery on site;	[32, 78, 79, 87, 89, 90, 94]
	Lightweight, less material use and less waste generation compared to site intensive construction;	[37, 75, 78, 79, 80, 87, 95, 96]
	Efficient land resource use. Foundation excavation is minimized and there are fewer potential wasteful site activities;	[78, 79, 87]
	Reduction in quantity of materials delivered on site with considerable economy of use in production than is achievable on site;	[78, 79, 87]
	Potential for waste management;	[79]
	Modular buildings can be easily reused or relocated at reasonable cost;	[75, 87, 93]
	Wider use of recycled materials (like timber, steel, aluminum, etc.) and greater opportunities for recycling in factory production;	[75, 78, 79, 80]

Table 2 to be continued

Social Benefits	Increase workforce health & safety;	[78, 79, 86, 91]
	Improved working conditions on site;	[32, 78, 84, 86]
	Reduced on-site risks by reducing elevated work and dangerous activities;	[32, 79, 84, 86]
	Excellent acoustic, thermal insulation and fire safety due to double skin nature of the construction, which means that each module is effectively isolated from its neighbours;	[75, 86]
	Health comfort and well-being of the occupants;	[75, 86]
	Affordability;	[86, 98]
	Reduced community disturbance;	[75, 78, 79, 86]
	Aesthetic options and beauty of the building;	[86]
	Influence of local social progress.	[86]

7. Conclusions

The construction sector needs more natural resources and generates more waste than any other industry in the world. These place the construction sector in the spotlight as changes in the design, construction, use and life cycle assessment of the sector can result in major improvements in the overall sustainability impact of the sector. Designing and constructing in the built environment with sustainability in mind can bring long-term benefits not only in terms of reduced material use and related environmental issues, but also in long-term economic and social wellbeing.

The potential for using modular construction is acknowledged by the construction sector. Technical, economic, and organizational factors currently hinder this potential from being utilized, rendering modular construction largely untapped. Despite the several initiatives to unlock modular construction, a lack of quantitative information restricts the demonstration of the real advantages to be gained. A key aspect that must be addressed in promoting modular construction is a change in the cultural mind-set towards this method of construction, and the wider collaboration between all actors involved in the planning, construction, maintenance, refurbishment of a modular building. Research that can better highlight the economic, environmental, social and technical benefits of modular construction would enable designers, contractors and real estate agents to get a better understanding of how changes in their current practices could be optimised through modular construction. Education and training in the wider skillset associated with modular construction, combined with the right policy incentives and opportunities for market development would empower their active participation in modular construction. This would provide the right conditions for modular construction to become a mainstream practice. In addition, political strategies that foresee the provision of incentives to boost modular construction, and the promotion of legislation for their usage, will help to realize the potential of this method as an alternative to traditional construction.

References

[1] Reeves, M. 2020. “Using Modular to Build for the Future.” *ASHRAE Journal* June 2020: 48-49 www.ashrae.org.

[2] McKean, J. 1994. *Crystal Palace*. London: Phaidon.

[3] Addis, B. 2006. “The Crystal Palace and Its Place in Structural History.” *International Journal of Space Structures* 21 (1): 3-19.

[4] Eiffel Tower Information: Facts, Height in Feet, Weight. Accessed February 10, 2021. toureiffel.paris.

[5] History of the Sears Catalog. Accessed February 10, 2021. searsarchives.com.

[6] Marquit, A., and Li, M. R. D. 2013. “From Sears and Roebuck to Skyscrapers: A History of Prefabricated and Modular Housing.” pp. 1-16.

[7] The History of Council Housing. Accessed February 10, 2021. uwe.ac.uk.

[8] “Prefabs updated”. Acocks Green Historical Society. Accessed February 10, 2021.

[9] Zachry, S., 2007. *21-Story Modular Hotel Raised the Roof for the Texas World Fair in 1968.* Charlottesville, VA: Modular Building Institute.

[10] Goulding, J., and Arif, M. 2013. *Off-site Production and Manufacturing—Research Roadmap Report.* International Council for Research and Innovation in Building and Construction. Accessed February 10, 2021. cibworld.nl.

[11] Alcorn, A. 2003. "Embodied Energy and CO_2 Coefficients for NZ Building Materials." Centre for Building Performance Research, Victoria University of Wellington.

[12] Allwood, J. M., Cullen, J. M., Milford, R. L. 2010. "Options for Achieving a 50% Cut in Industrial Carbon Emissions by 2050." *Environ. Sci. Technol.* 44: 1888-94.

[13] Allwood, J. M., Ashby, M. F., Gutowski, T. G., and Worrell, E. 2013. "Material Efficiency: Providing Material Services with Less Material Production." *Philos. Trans A Math. Phys. Eng. Sci.* 371: 20120496. doi: 10.1098/rsta.2012.0496.

[14] Giesekam, J., Barrett, J., Taylor, P., and Owen, A. 2014. "The Greenhouse Gas Emissions and Mitigation Options for Materials Used in UK Construction." *Energy and Buildings* 78: 202-14.

[15] Ness, D., Swift, J., Ranasinghe, D. C., Xing, K., and Soebarto, V. 2015. "Smart Steel: New Paradigms for the Reuse of Steel Enabled by Digital Tracking and Modelling." *Journal of Cleaner Production* 98: 292-303.

[16] DG Environment, European Commission. 2013. "BIO Intelligence Service, Sectoral Resource Maps." Prepared in response to an Information Hub request.

[17] Prism Environment. EU, 2012. "EISC, Construction Sector Overview in the UK."

[18] European Commission. 2014. *Communication from the Commission to the European Parliament, the Council, the European Economic and Social Committee and the Committee of the Regions on Resource Efficiency Opportunities in the Building Sector*. Brussels: COM, p. 445.

[19] Wahlström, M., Laine-Ylijoki, J., Järnström, H., Kaartinen, T., Erlandsson, M., Cousins, A. P., Wik, O., Suer, P., Oberender, A., Hjelmar, O., Birgisdottir, H., Butera, S., Astrup, T. F., and Jørgensen, A. 2014. *Environmentally Sustainable Construction Products and Materials—Assessment of Release and Emissions.* Oslo, Norway: Nordic Innovation.

[20] Crowther, P. 2014. "Investigating Design for Disassembly through Creative Practice." In *Proceedings of the Intersections International Symposium*, Santa Verdiana Church, Florence, Italy.

[21] EEA. 2012. *Material Resources and Waste—2012 Update. The European Environment—State and Outlook.* Copenhagen, Denmark: European Environment Agency (EEA).

[22] Heard, R., Hendrickson, C., and McMichael, F. C. 2012. "Sustainable Development and Physical Infrastructure Materials." *MRS Bulletin* 37: 389-94.

[23] Oikonomou, N. D. 2005. "Recycled Concrete Aggregates." *Cement Concrete Copmus*. 27: 315-8.

[24] Sabai, M. M., Cox, M. G. D. M., Mato, R. R., Egmond, E. L. C., and Lichtenberg, J. J. N. 2013. "Concrete Block Production from Construction and Demolition Waste in Tanzania." *Resource Conservation Recycling* 72: 9-19.

[25] BIO Intelligence Service. 2011. *Service Contract on Management of Construction and Demolition Waste: SR1. Final Report Task 2*. European Commission (DG ENV) Framework Contract ENV.G.4/FRA/2008/0112, Paris.

[26] Villoria Saez, P., del Río Merino, M., San-Antonio González, A., and Porras-Amores, C. 2013. "Best Practice Measures Assessment for Construction and Demolition Waste Management in Building Constructions." *Resource Conservation Recycling* 75: 52-62.

[27] Venables, T., Barlow, J., and Gann, D. 2004. *Manufacturing Excellence: UK Capacity in Off-site Manufacturing.* Innovation Studies Centre.

[28] Kamar, A. M., Hamid, Z. A., and Azman, N. A. 2011. "Industrialized Building System (IBS): Revisiting Issues of Definition and Classification." *International Journal of Emerging Sciences* 1 (2): 120.

[29] Oliveira, S., Burch, J., Hutchison, K., Adekola, O., Jaradat S., and Jones, M. 2017. *Making Modular Stack Up: Modern Methods of Construction in Social Housing.* Report Centre for Architecture and Built Environment Research, Department of Architecture and the Built Environment, University of the West of England.

[30] Ross, K. 2000. DETR *Construction Directorate Project Report: Advanced Of-fsite Production of Steel/Timber Building Systems.* Report on Market Survey 80-680 (Unpublished), BRE, Gaston, Watford.

[31] Lu, N. 2009. "The Current Use of Off-site Construction Techniques in the United States Construction Industry." In *Proceedings of Construction Research Congress, Building a Sustainable Future*, pp. 946-55.

[32] Blismas, N., and Wakefield, R. 2009. "Drivers, Constraints and the Future of Off-site Manufacture in Australia." *Construction Innovation* 9 (1): 72-83.

[33] Abosoad, H., Underwood, J., and Boveny, S. 2009. "Towards an Information System Representation of Off-Site Manufacturing (OSM) in Facilitating the Virtual Prototyping of Housing Design." In *Proceedings of the 9th International Postgraduate Research Conference (IPGRC)*, pp. 509-20.

[34] Azman, M., Ahamad, M., Majid, T., and Hanafi, M. 2010.

"The Common Approach in Off-Site Construction Industry." *Australian Journal of Basic and Applied Sciences* 4 (9): 4478-82.

[35] Goodier, C. I., and Gibb, A. G. 2005. "Barriers and Opportunities for Off-site in the UK. Systematic Innovation in the Management of Project and Processes." In *Proceedings of the CIB Helsinki International Joint Symposium*, pp. 148-58.

[36] Heather, L. 2003. *Modern Methods of House Building.* London: The Parliamentary Office of Science and Technology.

[37] Kawecki, L. R. 2010. "Environmental Performance of Modular Fabrication: Calculating the Carbon Footprint of Energy Used in the Construction of a Modular Home." Ph.D. thesis, Arizona State University.

[38] Haas, C. T., O'Connor, J. T., Tucker, R. L., Eickmann, J. A., and Fagerlund, W. R. 2000. *Prefabrication and Preassembly Trends and Effects on the Construction Workforce.* Report, Austin, TX: Center for Construction Industry Studies, University of Texas.

[39] Modular Building Institute (MBI) 2016. "Modular Advantage for the Commercial Modular Construction Industry." Charlottesville, Virginia.

[40] Mah, D. E. 2011. "Framework for Rating the Sustainability of the Residential Construction Practice." Ph.D. thesis, University of Alberta.

[41] Lawson, R. M., and Ogden, R. G. 2010. "Sustainability and Process Benefits of Modular Construction." In *Proceedings of the 18th CIB World Building Congress, TG57-Special Track*, May 10-13, 2010, Salford, UK, pp. 38-51.

[42] Na, L. 2007. "Investigation of the Designers' and General Contractors' Perceptions of Off-site Construction Techniques in the United States Construction Industry." Ph.D. thesis, Clemson University.

[43] NAHB. 1998. *Lean Construction*. Report, Marlboro, MD: National Association of Home Builders National Association of Home Builders.

[44] Celine, J. L. 2009. "The Evolution of the Use of Prefabrication Techniques in Hong Kong Construction Industry." Ph.D. thesis, Hong Kong Polytechnic University.

[45] McGraw-Hill, Construction. 2011. *Prefabrication and Modularization: Increasing Productivity in the Construction Industry.* Smart Market Report. New Orleans: McGraw-Hill Construction.

[46] Morton, J. 2011. "Going to Pieces over Modular Construction." *Buildings* 105 (12): 28-32.

[47] Said, H., Ali, A. R., and Alshehri, M. 2014. "Analysis of the Growth Dynamics and Structure of the Modular Building Construction Industry." In *Proceedings of the Construction Research Congress*, *ASCE*, May 19-21, 2014, Atlanta, Georgia, USA, pp. 1977-86.

[48] Ramaji, I., and Memari, A. 2015. "Information Exchange Standardization for BIM Application to Multi-story Modular Residential Buildings." In *Proceeding of the 6th Biennial Professional Conference, ASCE*, March 24-27, 2015, Milwaukee, Wisconsin, USA, pp. 13-24.

[49] Lawson, R. M., Ogden, R. G., and Bergin, R. 2012. "Application of Modular Construction in High-Rise Buildings." *Journal of Architectural Engineering* 18 (2): 148-54.

[50] Kozlovská, M., Kaleja, P., and Struková, Z. 2014. "Sustainable Construction Technology Based on Building Modules." *Advance Material Resources* 1041: 231-4.

[51] Haas, C. T., and Fagerlund, W. R. 2002. *Preliminary Research on Prefabrication, Pre-Assembly, Modularization and Off-Site Fabrication in Construction.* Austin, Texas: The Construction Industry Institute, The University of Texas at Austin.

[52] Quale, J., Eckelman, M. J., Williams, K. W., Sloditskie, G., and Zimmerman, J. B. 2012. "Construction Matters: Comparing Environmental Impacts of Building Modular and Conventional Homes in the United States." *Journal Ind Ecology* 16 (2): 243-53.

[53] Chiu, S. T. L. 2012. "An Analysis on the Potential of Prefabricated Construction Industry." Ph.D. thesis, The University of British Columbia.

[54] Schoenborn, J. M. 2012. "A Case Study Approach to Identifying the Constraints and Barriers to Design Innovation for Modular." M.Sc. thesis, Virginia Polytechnic Institute and State University.

[55] Buildoff-site. 2009. "Your Guide to Specifying Modular Buildings: Maximising Value and Minimising Risk." www.Build offsite.com.

[56] Mullen, M. A. 2011. *Factory Design for Modular Home Building*. Winter Park, FL: Constructability Press.

[57] National Audit Office. 2005. "Using modern Methods of Construction to Build More Homes Quickly and Efficiently."

[58] Cameron, P. J., and Di Carlo, N. G. 2007. "Piecing Together Modular: Understanding the Benefits and Limitations of Modular Construction Methods for Multifamily Development." M.Sc. thesis, Massachusetts Institute of Technology.

[59] Salama, T. 2018. "Optimized Planning and Scheduling for Modular and Off-site Construction." Ph.D. thesis, Concordia University.

[60] Azhar, S., Lukkad, M. Y., and Ahmad, I. 2013. "An Investigation of Critical Factors and Constraints for Selecting Modular Construction over Conventional Stick-Built Technique." *International Journal of Construction Education and Research* 9 (3): 203-25.

[61] Li, Z., Shen, G. Q., and Xue, X. 2014. "Critical Review

of the Research on the Management of Prefabricated Construction." *Habitat International* 43: 240-9.

[62] O'Connor, J. T., O'Brien, W. J., and Choi, J. O. 2016. "Industrial Project Execution Planning: Modularization versus Stick Built." *Practice Periodical on Structural Design and Construction* 21 (1): 04015014. doi: 10.1061/(ASCE)SC.1943-5576.000027004015014 .

[63] National Modular Housing Council (NMHC). 2017. *Builder's Guide to Modular Home Set-Up and Completion*. Report, Arlington, VA, USA. Assessed January 15, 2021. https://www.manufacturedhousing.org/wp-content/uploads/2017/01/Builders-Guide-to-Modular-Home-Set-Up-Completion.pdf.

[64] Wei, Y., Wang D. F., Liu, J. Y., Yu, C. L., Cheng, T., and Zhang, D. G. 2014. "Modularization Technology Development Prospects". *Applied Mechanics and Materials* 509: 92-5.

[65] McKinsey. 2019. *Capital Projects and Infrastructure, Modular Construction: From Projects to Products*.

[66] AGC. 2018. "2018 Workforce Survey Results." Associated General Contractors of America. https://tinyurl.com/ya9havyz.

[67] AGC. 2018. "Worker Shortage Survey Analysis." Associated General Contractors of America. https://tinyurl.com/yd7w3vhp.

[68] Sun, M., Sexton, M., Aouad, G., Fleming, A., Senaratne, S., Anumba, C., et al. 2021. *Managing Changes in Construction Projects.* Accessed January 15, 2021. http://www.builtenvironment.uwe.ac.uk/research/cprc/publications /mcd.pdf.

[69] Love, P. E., and Li, H. 2000. "Quantifying the Causes and Costs of Rework in Construction." *Construction Management Econ* 18: 479-90.

[70] Love, P. E., Mandal, P., and Li, H. 1999. "Determining the Causal Structure of Rework Influences in Construction." *Construction Management Econ* 17: 505-17.

[71] Hwang, B.-G., Thomas, S. R., Haas, C. T., and Caldas, C. H. 2009. "Measuring the Impact of Rework on Construction Cost Performance." *Journal Construction Engineering Management* 135: 187-98.

[72] Josephson, P. E., and Hammarlund, Y. 1999. "The Causes and Costs of Defects in Construction: A Study of Seven Building Projects." *Automation. Construction* 8: 681-7.

[73] Smith, G., and Jirik, T. *Making Zero Rework a Reality: A Comparison of Zero Accident Methodology to Zero Rework and Quality Management.* Research Report, Construction Industry Institute: Austin, TX, USA, pp. 203-11.

[74] Langdon, D., and Everest (now Aecom). 2004. "Cost Model of Off-Site Manufacture." *Building* 42: 67-72.

[75] Lawson, M., Ogden, R., and Goodier, C. 2014. *Design in Modular Construction.* Boca Raton, London, New York: CRC Press, Taylor & Francis Group.

[76] Rogan, A. L. 1999. *Building Design Using Cold Formed Steel Sections—Value and Benefit Assessment of Light Steel Framing in Housing.* Ascot, UK: Steel Construction Institute, p. 260.

[77] Rogan, A. L., Lawson, R. M., and Bates-Brkjak, N. 2000. *Value and Benefits Assessment of Modular Construction.* Ascot, UK: Steel Construction Institute.

[78] Ahna, Y. H., and Kim, K. T. "Sustainability in Modular Design and Construction: A Case Study of the Stack." *Int. Journal of Sustainable Building Technology and Urban Development* 5 (4): 250-9.

[79] Kamali, M., and Hewage, K. 2016. "Life Cycle Performance of Modular Buildings: A Critical Review." *Renewable and Sustainable Energy Reviews* 62: 1171-83.

[80] Jaillon, L., and Poon, C. 2010. "Design Issues of Using Prefabrication in Hong Kong Building Construction." *Construction Management and Economics* 28 (10): 1025-42.

[81] Gibb, A., and Isack, F. 2003. "Re-engineering through Pre-assembly: Client Expectations and Drivers." *Building Research & Information* 31 (2): 146-60.

[82] Edge, M., Craig, A., Laing, R., Abbott, L., Hargreaves, A., Scott, J., and Scott, S. 2002. "Overcoming Client and Market Resistance to Prefabrication and Standardization in Housing." Robert Gordon University, Aberdeen.

[83] Davies, A., Bagust, P., Basquill, M., 2018. "Modern Methods of Construction A forward-thinking solution to the housing crisis? Report for RICS. https://www.rics.org/globalassets/rics-website/media/news/news--opinion/modern-methods-of-construction-paper-rics.pdf

[84] Oliveira, S., Burch, J., Hutchison, K., Adekola, O., Jaradat, S., and Jones, M. 2017. "Making Modular Stack Up: Modern Methods of Construction in Social Housing." Report Centre for Architecture and Built Environment Research, Department of Architecture and the Built Environment, University of the West of England.

[85] Lu, N. 2007. "Investigation of the Designers' and General Contractors' Perceptions of Off-site Construction Techniques in the United States Construction Industry." Department of Career and Technology Education, Clemson University, Clemson, GA, USA.

[86] Kamali, M., and Hewage, K. 2017. "Development of Performance Criteria for Sustainability Evaluation of Modular versus Conventional Construction Methods." *Journal of Cleaner Production* 142 (4): 3592-606.

[87] Rogan, A. L., Lawson, R. M., and Bates-Brkliac, E. N.

2000. *Better Value in Steel: Value and Benefits Assessment of Modular Construction.* The Steel Construction Institute.

[88] Ferdous, W., Bai, Y., Ngo, T. D., Manalo, A., and Mendis, P. 2019. "New Advancements, Challenges and Opportunities of Multi-storey Modular Buildings—A State-of-the-Art Review." *Engineering Structures* 183: 883-93.

[89] Goulding, J., Rahimian, F. P., Arif, M., and Sharp, M. 2014. "New Off-site Production and Business Models in Construction: Priorities for the Future Research Agenda." *Architectural Engineering and Design Management* 11 (3): 163-84.

[90] Salama, T., Salah, A., Moselhi, O., and Al-Hussein, M. 2017. "Near Optimum Selection of Module Configuration for Efficient Modular Construction." *Automation in Construction* 83: 316-29.

[91] Ahn, S., Han, S., and Al-Hussein, M. 2016. "Recovery Time Analysis of Back Muscle Fatigue in Panelized Residential Modular Construction Factory." *Modular and Off-site Construction (MOC) Summit Proceedings* 1 (1): 224-31.

[92] Li, X. X., and Li, G. L. 2013. "Exploration of Modular Build of Architectural Space." In *Applied Mechanics and Materials*. Zurich, Switzerland: Trans Tech Publications Ltd., pp. 338-44, 357.

[93] Lu, N., and Korman, T. 2010. "Implementation of Building Information Modeling (BIM) in Modular Construction: Benefits and Challenges." In *Construction Research Congress: Innovation for Reshaping Construction Practice*, pp. 1136-45.

[94] Amiri, A., Caddock, P., and Whitehead, M. 2013. "Accounting for the Greenhouse Gas Emissions of Construction: A UK Case Study." *Proceedings of the Institution of Civil Engineers-Civil Engineering* 166 (2): 82-8.

[95] Illankoon, I. C. S., and Lu, W. 2020. "Cost Implications of Obtaining Construction Waste Management-Related Credits in Green Building." *Waste Management* 102: 722-31.

[96] Wang, J., Li, Z., and Tam, V. W. 2014. "Critical Factors in Effective Construction Waste Minimization at the Design Stage: A Shenzhen Case Study, China." *Resources, Conservation and Recycling* 82: 1-7.

[97] Ambler, S. 2013. "Briefing: Off-Site Construction of a New Nuclear Laboratory at Dounreay, Scotland." *Proceedings of the Institution of Civil Engineers-Energy* 166 (2): 49-52.

[98] Thompson, J. "Modular Construction: A Solution to Affordable Housing Challenges." *Cornell Real Estate Review* 17, Article 21. https://ecommons.cornell.edu/bitstream/handle/1813/70841/18_Modular_Construction_A_Solution_to_Affordable_Housing.pdf?sequence=1&isAllowed=y.

Journal of Civil Engineering and Architecture 15 (2021) 330-341
doi: 10.17265/1934-7359/2021.06.005

Urban Forest Digital Cadastre

Nicola Noe[1] and Federico Massi[2]

1. School of Architecture Urban Planning Construction Engineering, Politecnico Milano 1863, Piazza Leonardo da Vinci, 32, Milan 20133, Italy

2. Dipartimento di Scienze Agrarie e Ambientali, Università degli Studi di Milano, Via Celoria 2, Milan 20133, Italy

Abstract: Urban forests being part of the Natural Capital, they provide goods and services for humans, the ecosystem services that are necessary for their survival. Over recent years, the importance of ecosystem services within urban landscapes has grown steadily. Determining the amount and the value of the ecosystem services provided by the Urban Forest is the main goal of the "Digital Green Cadastre" (DGC), a project in progress of survey, classification and mapping of the urban, agricultural and natural green assets. The DGC records the types of green cover and soil characteristics and utilizes the calculation of the total leaf area for the quantitative analysis of the botanical heritage, environmental performance and ecosystem benefits, such as water runoff management, air pollutant removal and urban heat island reduction. The case study of Abbiategrasso—a small town in Italy—is reported.

Key words: Natural capital, ecosystem services, urban forests, DGC, leaf area index (LAI).

1. Introduction

The Natural Capital is the entire stock of natural assets, living organisms, air, water, soil and geological resources, which provides goods and services—directly or indirectly—for humans and that are necessary for their survival. The flows of goods and services that the Natural Capital offers daily and from which humans benefit are indicated by the term ecosystem services [1]. In recent years, the importance of ecosystem services within urban landscapes has grown steadily [16]. The percentage of people living in cities has increased from about 10 to over 50% in just a few decades [3] and urbanization will continue to shape the future, as new population growth is predicted to take place in urban areas. More than 60% of the total population is expected to live in cities by 2030 [17]. Supporting the well-being of urban populations requires a steady and growing flow of natural resources imported from rural areas, as well as the natural areas needed to treat the waste generated by cities. Ecological footprint analysis documents that this may require non-urban land hundreds of times larger than the area of the city itself [13, 14]. The cities ecological footprint is enormous and the extent to which cities can sustain themselves in even a limited number of ecosystem functions is likely to continue to decline over the next decade. The evolution of this negative trend is accelerated by the growing problems deriving from climate change and by the proliferation of land management models that are putting sustainability at risk, entailing—among others—phenomena of soil consumption and progressive qualitative decline, with heavy environmental, economic and social repercussions [10].

A new model of economic and social development and a new land management model in the cities are thus required. Urban forestry emerged in North America in the 1960s as an innovative model for urban natural resource management [7]. Urban forestry has since evolved to quantify the structure, function and value of urban trees [8, 11], applying forest ecology and ecosystem management concepts to urban trees [15, 12]. Now it is common for large cities to set general urban forestry plans to optimize tree selection criteria, estimate total urban canopy

Corresponding author: Nicola Noe, PhD, agronomist, adjunct professor of "botany and arboriculture", research fields: green spaces in urban environments, plant nutrition, small fruits, tissue cultures and urban and sport lawns.

coverage and provide long-term goals such as water runoff management, increase in the value of rainwater and urban heat island reduction [6, 12].

Ecosystems designed by urban forestry are one of the most important ecosystem service providers for the world's population. However, they are largely left out of decision making in urban area management, due to the general lack of awareness of how the ecosystem services associated with these systems can be quantified. The failure to give a value to Urban Forests—and related ecosystem services provided—is largely due to ignorance of their value to human well-being and to inadequate socioeconomic valuation mechanisms. To support the choices of planning and management of the territory, it is thus necessary to look for indicators to measure the landscape, naturalistic and environmental functions that plants exert through their hypogeal and epigeal apparatuses. Identification and collection of such indicators enables us both to calculate the ecological benefits and to compare different landscape, urban planning and territorial solutions in terms of the value of the ecosystem services provided [9].

Many products are available for the acquisition and management of Urban Forests data, in particular concerning the management of it. Conversely, there is much less to the acquisition of data aimed at determining the environmental performance of the Urban Forests. To help complete this fundamental step in the process of determining the value of the Urban Forests, from 2014 the "Digital Green Cadastre" platform (hereafter "DGC") is being studied, a project in progress of survey, classification and mapping of the urban green cover, agricultural and natural heritage (http://www.catastodelverde.it) (Fig. 1).

2. Material and Methods

2.1 The IT Structure of the DGC

The DGC platform for the management of urban green information is based on two software pillars that are appropriately put together:

(1) The Google Maps platform, which offers extremely sophisticated geographic information systems (GIS) management procedures—web services in API (application programming interface) mode—and provides a photogrammetric detailed mapping of the entire Italian territory, as well as the Street View overviews of almost all national roads, usable in green survey and mapping.

(2) A spatial geographic database set up on the MongoDB database, which allows particularly complex spatial queries and can guarantee the management of a substantial information asset, always in scalable web mode.

The DGC information set is divided into three classes of objects:

(1) Administrative Zones[1]: define a specific zoning (municipal perimeter of green areas, cadastral parcels, area and basin perimeters, zoning of regulatory plans …).

(2) Surfaces: include all the green surfaces or in any case referable to the green management chapter (woods, cultivated land, lawns, shrubbery, uncultivated land, horizontal and vertical green surfaces on buildings ...).

(3) Punctual objects: include all the botanical entities and the elements related to the theme of green management, which have a precise localization (trees, shrubs, games, benches, poles, fountains ...).

The DGC is geometric in nature. Each registered entity has its own spatial component related to the alphanumeric information component. In addition to absolute data on the specific botanical or dimensional characteristics of the species, punctual objects and

[1] The "Administrative Zones" are space objects that in many cases can be derived and not managed internally in the Land Registry. The municipal boundaries, the cadastral parcels and the zoning of the General Town Development Plan are examples of Administrative Zones that may not be duplicated within the DGC. Unlike the boundaries and the codes of the green areas imposed by the offices for administrative and accounting needs, they are zones that find in the Green Cadastre the most suitable place for their memorization and management.

Fig. 1 The "Digital Green Cadastre" website (http://www.catastodelverde.it).

surfaces, the DGC also records historical data of maintenance, diagnostic and phytosanitary interventions. The three classes of objects are autonomous and unrelated to each other—if not spatially—or with respect to the absolute localization on the map.

2.1.1 Logical Structure of the "Administrative Zones"

The "Administrative Zone" object represented in JSON format, consists of an "_id" identifier, a job parameter that identifies belonging to a cluster, an area, a reference municipality, and a GeoJSON format representation of an area object containing a series of "properties".

These properties are free in their number and in their definition:

• If for example the administrative area is the cadastral theme, the 3 properties that will indicate a single particle within the "Codice Belfiore"[2] are: "Foglio", "Particella" and "Subalterno".

• If the zone is a subdivision of areas for maintenance, there will probably be at least one identifying field with the code or the name of the zone.

• If the area is the organization by districts of the municipality, there will be a field indicating the number or name of the neighborhood.

The administrative zones can be more than one for each project, and only serve to localize an area and create clusters for territorial statistical operations (i.e. how many plants per area, how much lawn for each neighborhood, which species and quantity of plants by species in a park).

Each single node of the network of servers that make up the DGC can choose to encode these areas and make them available to other nodes so that users can use them for their selections.

Between Administrative Zone and Surfaces and/or Punctual Objects there is a dynamic spatial relationship that is not recorded and maintained between the properties of each individual object. The rule according to which this plant belongs to this flower bed arises from the topological relationship of the precise object "plant" which is spatially contained

[2] The Belfiore Code is the Italian National Code (also called: cadastral administrative code or, improperly, Cadastral Code) and is a unique identification code assigned to each Italian Municipality and foreign state.

in the object area "flower bed", and not thanks to a supposed field "zone" in the definition of the parameters that define plant object.

2.1.2 Logical Structure of the "Surfaces"

The "Surface" object represented in JSON format consists of an "_id" identifier, a job parameter that identifies belonging to a context, an area, a reference municipality, and a GeoJSON format representation of an area object containing a series of "properties":

- Genus and Species List (area general): The list of botanical species is taken from any Trees & Shrubs searchable database in REST web service mode, and for which the specifications for free use are provided.
- Area Class List (classe_area): Full Soil, Green Roof, Green Wall, Flowerpot, Waterproof Surface …
- Area Type List (area_type): Sand Mixture, Asphalt, Playground, Self-locking paving, Bare soil, Driveway lawn, Lawn, Group of trees, Group of shrubs, Hedge, Ground Cover Plants …
- Event Type List (type): Pruning, Damage, Phytopathology/Pests, Tree measurements, Planting, Tree Felling, Fertilization, Lawn cutting, Leaves collection …

2.1.3 Logical Structure of "Punctual Objects"

The object "Punctual Object" represented in JSON format consists of an identifier "_id", a job parameter that identifies belonging to a context, an area, a reference municipality, and a representation in GeoJSON format of a punctual object containing a series of "properties":

- Aggregation List (status): Group, Row, Isolated …
- Growth Habitus List (veg): Tree, Shrub …
- Event Type List (type): Pruning, Damage, Phytopathology/Pests, Tree measurements, Planting, Tree Felling, Fertilization …

One of the most relevant objectives of the DGC is to determine the ecological and economic value of ecosystem services provided by Urban Forests. Given the complexity of acquiring precise data, the objective of determining the value of the ecological benefits provided by the plants does not necessarily need to be pursued through the direct measurement of the individual environmental performance, but can be achieved through an estimate of the value of ecosystem services, with an approach by categories and models. In this sense, it is noticeable that some of the most important ecosystem services provided by plants are related to the extension of the leaf apparatus [4, 5]: from the outflow of rainwater to the removal of air pollutants, to the heat absorbed by evapotranspiration, to the reduction of CO_2 and the production of O_2 through the photosynthetic process [9].

The DGC quantifies selected ecosystem services starting from a parameter such as the size of the foliage—in its two-dimensional expression of the projection—and then transforming it into economic value as savings on the management.

The crown projection is a measure that is obtained with acceptable approximation through the interpretation of the aerial photographs. The crown projection, expressed on the surface, multiplied by the leaf area index (LAI) provides an estimate of the Leaf Area for each plant or for groups of plants.

Nevertheless LAI is a complex index to calculate because it depends on numerous factors, from species to growth stage, from soil conditions to microclimate conditions, from maintenance to phytosanitary status, etc. Therefore for the specific purposes a mean LAI has been adopted for each type of plant cover, lawn, shrub and tree, also determining sub-categories to consider the intermediate conditions (Table 1). The DGC uses the average LAI expected for typology of green cover which ranges from 0 of the bare ground to 18 of some conifers. Being a relationship between two surfaces, LAI represents a pure numerical parameter; it is therefore dimensionless, being measured in m^2/m^2. LAI therefore represents the amount of leaf material in an ecosystem and is geometrically defined as the total one-sided area of photosynthetic tissue per unit ground surface area [2].

Total leaf area (m^2) = Crown projection (m^2) × LAI

Table 1 LAI applied in the DGC for typology of plant cover.

LAI	Typology of plant cover
0	Bare ground
0.2	Almost bare ground
0.5	Very degraded lawn, armed lawn with self-locking devices
0.8	Slightly degraded lawn
1.0	Lawn in fairly vegetative state, extensive meadows and natural areas (cuttings < 3)
1.2	Non-irrigated lawn in fairly vegetative state (cuttings 3-6)
1.5	Irrigated lawn in good vegetative state (cuttings 6-10)
2.0	Valuable irrigation lawn and sports turf (cuttings > 10)
2.8	Carpeting shrubs (plant density > 10 p/m^2)
3.0	Small shrubs (plant density 3-10 p/m^2)
3.2	Medium-sized shrubs (plant density 1-3 p/m^2)
3.5	Large bushes (plant density < 1 p/m^2)
4-6	Isolated broad-leaved deciduous trees: small-size trees, columnar trees or trees maintained with short pruning
5	Broad-leaved deciduous wood
6-7	Isolated broad-leaved deciduous trees: medium-size trees, large columnar trees or large trees maintained with short pruning
7-8	Isolated medium-size broad-leaved evergreen trees
7	Deciduous needle-leaved wood
8	Isolated large broad-leaved deciduous trees
9	Evergreen needle-leaved wood
10	Isolated evergreen broad-leaved large trees
12-14	Isolated evergreen needle -leaved large trees

A further refinement of the data can be obtained by introducing an index of vigour that takes into account the state of health of the crown. The Index of Plant Vigour (IPV) ranges from 0 of the almost dead tree to 1 of the healthy plant. Therefore, given the same species and crown projection, a different total leaf area may correspond.

Total leaf area (m^2) = Crown projection (m^2) × LAI (from DB) × IPV

The amount of the tree leaf area has been used:

- to estimate the volume of meteoric water intercepted by the canopy before reaching the ground; this value provides the basis for all the outflow calculations and, ultimately, savings for adaptation and maintenance of the sewage system;
- for the evaluation—through simulation models—of the amount of energy in kWh implied by the presence of vegetation;
- to calculate the interception surface of pollutants, providing the basis for estimating to removal of pollutants present in the atmosphere or dissolved in meteoric waters;
- to calculate the quantity of photosynthesizing tissue, providing the basis for estimating the reduced CO_2 quantity in the photosynthesis process.

In the present survey, the ecosystem services provided by plants have been estimated with reference to USDA Forest Service's i-Tree™ (https://www.itreetools.org/)[3] and expressed in terms of savings in the management cost for rainwater interception, microclimate mitigation, air pollutants removal and CO_2 reduction.

2.2 Data-Entry in Abbiategrasso (Milan, Italy)

The DGC was applied for the first time in 2014 in the municipality of Abbiategrasso, where the following updates of the project were tested (Fig. 2).

[3] USDA Forest Service's i-Tree™ (https://www.itreetools.org/) is a set of free tools built on science that quantifies the benefits and values of trees around the world, aids in tree and forest management and advocacy, shows potential risks to tree and forest health and is based on peer-reviewed, USDA Forest Service Research in the public domain.

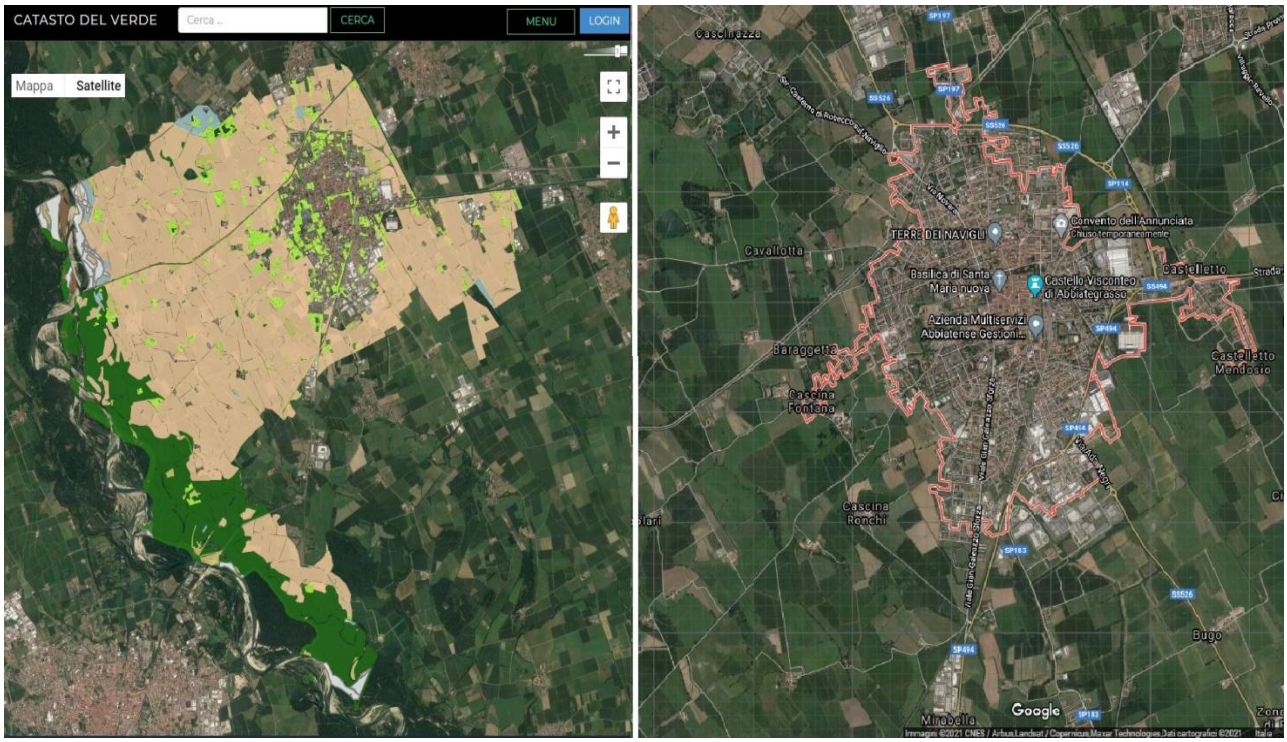

Fig. 2 Abbiategrasso municipality boundaries on the left (dark green: naturalistic, yellow: agricultural, pale green: urban and gardens) and Abbiategrasso City boundaries on the right; from the "Digital Green Cadastre" website (http://www.catastodelverde.it) and Google Maps.

2.2.1 Administrative Data

- Area Code (given automatically by the software).
- Green Space Category (Gardens, Parks, Lawns, Road Green, Extensive Green, Residential Green, Playgrounds, Dogs Area, Sports Area, Parking Area, Vegetable Gardens, Cemetery Green, Green Roofs, Green Walls, Uncultivated Areas, Woodland, Shrubs and Shrubland, Orchards, Vineyards, Wood Arboretum, Waterway Banks, Arable Land, and others).
- Ownership (Public/Private).
- Management (Public/Private/Private for public use).
- Maintenance (Enter name of the Company).

2.2.2 Area Data

- Area Surface.
- Soil characteristics (Full Soil, Green Roof, Green Wall, Flowerpot, Waterproof Surface).
- Types of surface cover (Mineral/Vegetal).
- Types of mineral material (Asphalt, Decomposed Granite, Self-binding Limestone, Self-binding Gravel, Sand Mixture, Playground, Self-locking Paving).
- Types of vegetation cover (Trees in row, Trees in group, Woodland i.e. Trees in group surface > 2,000 m^2, Shrubs in group, Hedge, Ground Cover plants, Lawns, Bare ground).
- Lawns: non-irrigated extensive lawn (No. of cuts < 3), non-irrigated lawn (3-6 cuts), irrigated ornamental lawn (6-10 cuts), fine irrigated ornamental lawn (No. of cuts > 10), irrigated sports turf (No. of cuts > 10), non-irrigated sports turf (No. of cuts > 10).
- Ground Cover Plants: planting layout < 10 plants/m^2, > 10 plants/m^2.
- Shrubs in group: planting layout < 1 plant/m^2, > 1 plant/m^2.
- Trees in group: planting layout 1-3 plants/100 m^2, 3-10 plants/100 m^2, > 10 plants/100 m^2.
- Vegetation cover height (m).
- Ground cover vegetation genus and species or type (pre-digit enter from any Shrub & Trees database).

• Events/Notes: date and operation (Pruning, Damages, Phytopathology-Pest, Plant height, Planting, Plant removal, Fertilization, Lawn cutting, Leaf collection, and others).

2.2.3 Punctual Data (Tree/Shrub)

• Object number (given automatically by the SW).
• Status (Group/Row/Isolated).
• Habitus (Tree/Shrub/Other).
• Genus and Species (pre-digit enter from any Shrub & Trees DB).
• Height (m).
• Trunk diameter (cm).
• Crown diameter (m).
• Events/Notes: date and operation (Planting, Fertilization, Lawn cutting, Leaf collection, Pruning, Suckering, Damages, Phytopathology/Pest, VTA Class, Plant height, Trunk diameter, Crown diameter, Tree removal, and others).

3. Results and Discussions

The city of Abbiategrasso was used as a test area of the DGC.

The polygons of the public green areas in charge of the public administration and related characteristics have been inserted into the platform, followed by the areal elements (lawns, trees and shrubs in groups) and punctual elements (isolated trees and shrubs) (Fig. 3).

The Green Balance Sheet of the public urban forest of Abbiategrasso in charge of the Municipal Administration (http://www.urbanplan.it/amaga/#) can be generated in real-time by clicking "STAT." on and then "SCHEDE BILANCIO DEL VERDE". The results of the data uploaded to the platform up to March 2021 are reported and analyzed (Fig. 4).

General Data (Census data)	
Population	32,537
Abbiategrasso total surface (m^2)	47,805,402
Built surface (m^2)	1,758,966
Road surface (m^2)	1,632,990
Surface with vegetation (m^2)	44,413,446
Composition of green surface	
Agricultural (m^2)	26,240,819
Naturalistic (m^2)	7,554,037
Urban* (m^2)	1,524,000
Urban Green Surface per inhabitant (m^2)	46.76

* estimated

Fig. 3 Abbiategrasso (Milan, Italy) (http://www.urbanplan.it/amaga/#).

Fig. 4 Urban green areas under investigation.

4. Urban Green Data (from DGC)

The Urban Green areas in charge of the administration and object of the present survey are shown in Fig. 4. They have a total surface of 723,972 m^2 and 552,911 m^2 are classified "lawns" as far as management is concerned with 67.2% in the class of "Extensive lawns", low maintenance lawns requiring less than 3 cuts per year (Table 2).

Within these areas 6,535 isolated trees are counted in total. Trees belonging to the following 15 genus represent 90.52% of the population as follows: Tilia 19.35%, Acer 9.87%, Populus 9.04%, Prunus 7.85%, Platanus 7.38%, Aesculus 7.12%, Celtis 5.97%, Cedrus 4.20%, Quercus 4.01%, Pinus 3.69%, Fraxinus 3.62%, Ailanthus 2.46%, Robinia 2.06%, Lagerstroemia 1.95%, Liquidambar 1.95%. The remaining 9.48% is divided into the following genus: Betula, Fagus, Carpinus, Ulmus, Picea, Magnolia, Sophora, Abies, Albizia, Cupressus, Chamaecyparis, Morus, Taxus, Acacia, Araucaria, Eriobotrya, Hibiscus, Ilex, Juglans, Laurus, Ligustrum, Liriodendron, Olea and Punica.

The great proportion of trees and shrubs are broad-leaved deciduous, respectively 88.0% and 78.0%. The difference is a higher proportion of broad-leaved evergreen shrubs (12%) in comparison to broad-leaved evergreen trees (2%) (Table 3). The preponderant size class (Fig. 5) of tree population is the 2nd (63%) and with respect to tree species origin (Fig. 6) 52% of the trees are from naturalized species. The actual class diameter and height are in Tables 4 and 5.

Table 2 Lawns.

Extensive lawn (No. of cuts < 3)	67.2%
Extensive lawn (No. of cuts 3-6)	29.4%
Ornamental lawn (No. of cuts 6-10)	3.2%
Fine ornamental lawn (No. of cuts >10)	0.1%
Sports turf (No. of cuts > 10)	0.1%

Table 3 Trees and shrubs.

	Trees	Shrubs
Deciduous broad-leaved	88.0%	78.0%
Evergreen broad-leaved	2.0%	12.0%
Deciduous conifers	1.0%	1.0%
Evergreen conifers	9.0%	9.0%

Table 4 Tree trunk circumference.

< 50 cm	9.31%
50-100 cm	86.51%
100-200 cm	3.22%
200-300 cm	0.76%
> 300 cm	0.16%

Table 5 Tree height.

< 6 m	83.06%
6-12 m	12.19%
12-20 m	4.59%
20-30 m	0.12%
> 30 m	0.03%

Table 6 Total leaf area.

Plant cover (canopy)	m^2	%
Lawns	540,064	35.17
Isolated trees	842,544	54.87
Trees in row	93,496	6.09
Trees in group	37,445	2.44
Woods	16,865	1.10
Isolated shrubs	354	0.02
Shrubs in group	520	0.03
Hedges	3,894	0.25
Ground covering shrubs	293	0.02
Bare ground	164	0.01
Total	1,535,639	

The DGC calculates the total leaf area using the surfaces of the lawn areas and the projection of the foliage of trees and shrubs multiplied by the LAI according to Table 1. The estimated total leaf area is 1,535,639 m^2 (Table 6). Trees contribute for about 58% of the total leaf area (Fig. 7).

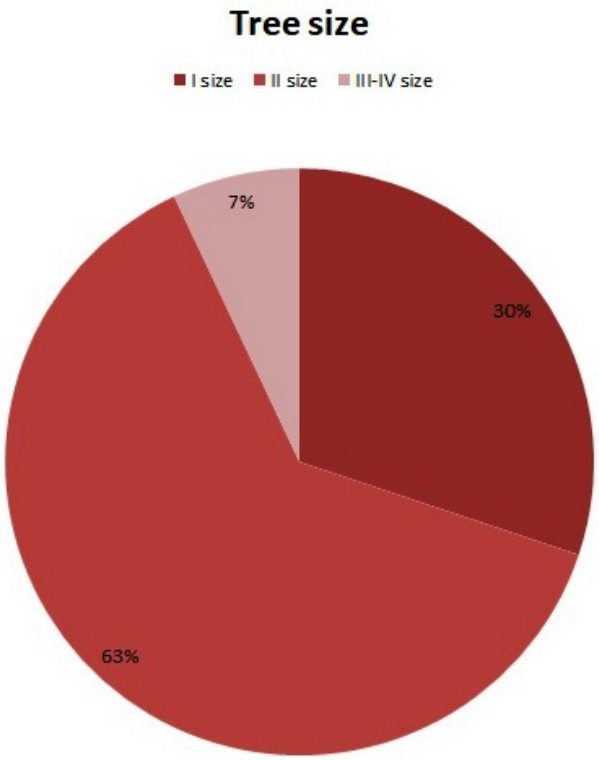

Fig. 5 Dimensional class (expected growth: I = very large tree species, IV = small tree species).

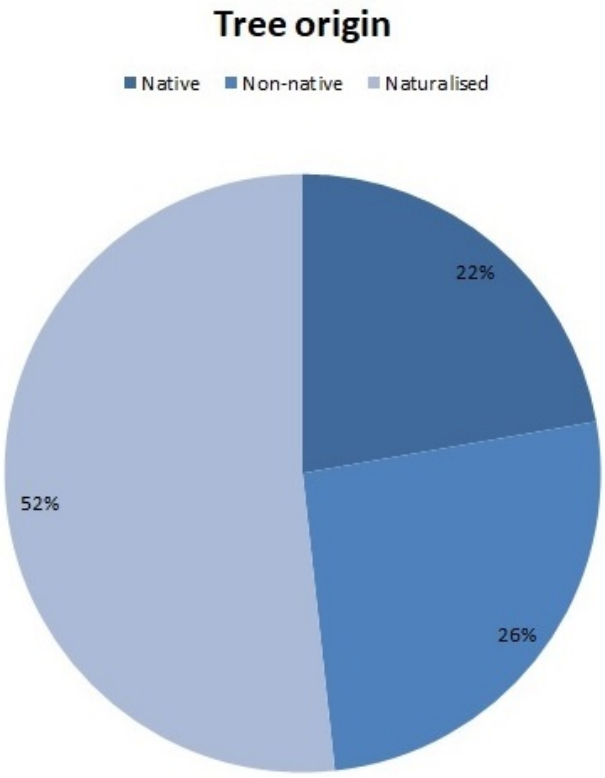

Fig. 6 Tree species origin.

Table 7 Total leaf area.

	Ecosystem services per year	Savings per year
Stormwater interception, runoff management	85,422 m^3	€203,303.49
Air pollutants removal	15,074 kg	€149,538.11
Micro-climate mitigation, heath absorbed by evapotranspiration	18,424,274 kWh	€2,026.670.14
CO_2 fixed	5,024,802 kg	€33,314.44
Total		€2,412,826.17

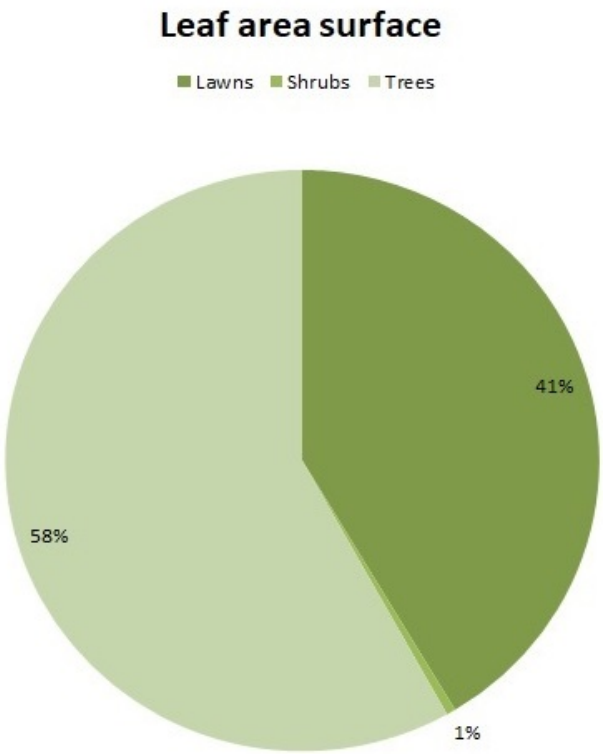

Fig. 7 Leaf area surface.

In Table 7 some of the benefits related to the total leaf area of herbaceous, shrub and tree plants area reported. The DGC estimation is as follows: 85,422 m^3/year of stormwater interception, 15,074 kg/year of air pollutants removal, 18,424,274 kWh/year of equivalent heath absorbed by evapotranspiration and 5,024,802 kg/year of CO_2 reduced. The environmental effects are economically evaluated in terms of yearly savings on city management as follows: runoff management €203,303.49, air pollutants removal €149,538.11, micro-climate mitigation €2,026,670.14 and CO_2 removal €33,314.44.

5. Conclusions

The DGC is a project of survey, classification and mapping of the public and private urban, agricultural and natural urban forest, which introduces some important elements of originality and innovation.

The DGC has moved from a quantitative analytical criterion to a systematic performance model that has taken as a first reference the ecosystem control of green facilities, overcoming the computational/taxonomic criterion in favour of the formation of final balances and the monitoring of evolutionary dynamics of the urban forest.

The DGC was therefore shown:

- to be an easy application tool for the acquisition of botanical data and able to use the most up-to-date survey and data processing technologies;
- to recover the censuses performed with traditional methodology and the measurement of the urban forest;
- to deal with other territorial databases;
- to produce a quantitative balance of public and private urban forest, standardized at national level, in response to the increasingly pressing demands of environmental quality, in particular urban;
- to calculate the quantity and economic value of the ecosystem services provided by the urban forest;
- to support the choice of development models that recognize the environmental and economic value of the urban forest and the soil, through the estimate of the asset value of the urban forest;
- to keep alive the botanical data collected daily in the area.

The novelty of the DGC approach does not lie in the IT management and the sharing and publication on the web of data—which is based on procedures already widely tested and successfully applied in other

contexts—but in identifying the performance parameters and the classification model able to constitute a reference standard for the municipal urban green balance [9].

The DGC project identifies in the measurement of the total leaf area one of the main parameters for the quantitative analysis of the botanical heritage, environmental performance and ecosystem benefits. Using the Leaf Area as the parameter for the measurement of the botanical heritage and of the ecosystem benefits makes it possible, for example, to estimate with acceptable approximation the quantity of urban greenery. This parameter can be used for a single plant, but also for larger surfaces covered by vegetation, in order to measure radically different situations in terms of ecosystem services provided.

The Abbiategrasso Urban Forest data uploaded on the DGC have been used to produce on-time the Green Balance. The Green Balance is crucial for evaluating not only the amount but—most of all—the environmental performances of the urban forest. A very interesting consideration is that, with an annual cost of maintenance of the public botanical heritage of around €800,000.00, including leaves collection, the botanical heritage generates a multiplicity of ecosystem benefits that should be equally monetized. On the basis of bibliographic data deriving from studies that are multiplying in many cities of the world, the DGC calculates the value of four ecosystem benefits linked to the total leaf area in terms of saving on the management of rainwater, reduction of air pollutants, energy consumption for air conditioning of buildings and CO_2 removal, which amounts to about €2,400,000.00 per year.

The format of the Green Balance can be tailored to the requirements of the administration or other stakeholders.

Acknowledgments

The project would never have come to life without the support of Magellano Progetti (http://www.magellanoprogetti.com/) and Urbanstudio (http://www.urbanstudio.it/).

References

[1] Costanza, R., d'Arge, R., de Groot, R., Farber, S., Grasso, M., Hannon, B., Limburg, K., Naeem, S., O'Neill, R. V., Paruelo, J., Raskin, R. G., Sutton, P., and van den Belt, M. 1997. "The Value of the World's Ecosystem Services and Natural Capital." *Nature* 387: 253-60.

[2] Gobron, N., and Verstraete, M. 2009. "FAPAR, ECV-T11: GTOS Assessment of the Status of the Development of Standards for the Terrestrial Essential Climate Variables." Presented at ECV-T11, FAO, Rome.

[3] Grimm, N. B., Faeth, S. H., Golubiewski, N. E., Redman, C. L., Wu, J., Bai, X., and Briggs, J. M. 2008. "Global Change and the Ecology of Cities." *Science* 319: 756-60.

[4] Hardin, P. J., and Jensen, R. R. 2007. "The Effect of Urban Leaf Area on Summertime Urban Surface Kinetic Temperatures: A Terra Haute Case Study." *Urban Forestry and Urban Greening* 6: 63-72.

[5] Kaufmann, M. R., and Troendle, C. A. 1981. "The Relationship of Leaf Area and Foliage Biomass to Sapwood Conducting Area in Four Subalpine Forest Tree Species." *Forest Science* 27 (3): 477-82.

[6] Konijnendijk, C. 2003. "A Decade of Urban Forestry in Europe." *For Policy and Economy* 5 (2): 173-86.

[7] Konijnendijk, C., and Gauthier, M. 2006. "Urban Forestry for Multifunctional Land Use." In *Cities Farming for the Future: Urban Agriculture for Green and Productive Cities*, edited by Van Veenhuizen, R. Ottawa: International Development Research Centre. Accessed Dec. 2012. http://www.idrc.ca/en/ev-103884-201-1-DO_TOPIC.html.

[8] Maco, S. E., and McPherson, E. G. 2003. "A Practical Approach to Assessing Structure, Function, and Value of Street Tree Populations in Small Communities." *J Arboric* 29 (2): 84-97.

[9] Noe, N. 2019. *The Digital Green Cadastre—Open Data and Ecosystem Services*. Lambert Academic Publishing (LAP).

[10] Noe, N., and Stefanello, V. 2020. "Emergenza planetaria, emergenza ambientale." In *Manifesto per la difesa del verde in ambito urbano in Italia nel dopo Covid-19—Gli altri contributi*, 5-6. https://www.ilverdeeditoriale.com/pdf/Manifesto_altri_contributi.pdf.

[11] Nowak, D. J. 2006. "Institutionalizing Urban Forestry as a 'Biotechnology' to Improve Environmental Quality." *Urb for Urb Green* 5: 93-100.

[12] Nowak, D. J., and Dwyer, J. F. 2007. "Benefits and Costs of Urban Forest Ecosystems." In *Urban and Community Forestry in the Northeast*, edited by Kuser, J. E.

Netherlands: Springer, 25-46.

[13] Rees, W. E. 1992. "Ecological Footprints and Appropriated Carrying Capacity: What Urban Economics Leaves Out." *Environ Urb* 4 (2): 121-30.

[14] Rees, W. E., and Wackernagel, M. 1996. "Urban Ecological Footprints: Why Cities Cannot Be Sustainable—and Why They Are a Key to Sustainability." *Environ Impact Assess Rev* 16: 223-48.

[15] Rowntree, R. A. 1998. "Urban Forest Ecology: Conceptual Points of Departure." *J Arboric* 24 (2): 62-70.

[16] Schwarz, N., Moretti, M., Miguel, N., Bugalho, Z., Davies, G., Haase, D., Hack, J., Hof, A., Melero, Y., Pett, T. J., and Knapp, S. 2017. "Understanding Biodiversity-Ecosystem Service Relationships in Urban Areas: A Comprehensive Literature Review." *Ecosystem Services* 27: 161-71.

[17] United Nations. 2004. *World Urbanization Prospects: The 2003 Revision*. New York: United Nations.

Journal of Civil Engineering and Architecture
Volume 15, Number 6, June 2021
David Publishing Company
3 Germay Dr., Unit 4 #4651, Wilmington DE 19804, USA
Tel: 1-323-984-7526; Fax: 1-323-984-7374
http://www.davidpublisher.com, www.davidpublisher.org
civil@davidpublishing.com, civil@davidpublishing.org, civil_davidpublishing@yahoo.com

ISSN 1934-7359
06
9 771934 735214